Chemical Geology 513 (2019) 167–183

Contents lists available at ScienceDirect

Chemical Geology

journal homepage: www.elsevier.com/locate/chemgeo

Refining the interpretation of lacustrine carbonate isotope records: Implications of a mineralogy-specific Lake Van case study

Jeremy McCormack[a,*], Gernot Nehrke[b], Niels Jöns[a], Adrian Immenhauser[a], Ola Kwiecien[a]

[a] Department of Geology, Mineralogy and Geophysics, Ruhr University Bochum, 44801 Bochum, Germany
[b] Alfred Wegener Institut, Helmholtz Zentrum für Polar und Meeresforschung, 27570 Bremerhaven, Germany

ARTICLE INFO

Editor: E. B Michael

Keywords:
Oxygen and carbon isotopy
Lake Van
Aragonite and calcite
Diagenetic dolomite
Palaeoenvironmental reconstructions

ABSTRACT

Oxygen and carbon isotope ($\delta^{18}O$ and $\delta^{13}C$) data from bulk carbonates are widely applied proxies for temperature, the precipitation/evaporation ratio and productivity in lacustrine palaeohydrology and palaeoclimatology. In case of the terminal and alkaline Lake Van, however, previous studies have shown that bulk oxygen isotope compositions are in disagreement with other proxies when interpreted in a conventional manner. Similarly, the reports on the nature and the timing and site of carbonate precipitation in Lake Van are inconsistent. This study provides evidence on the mineralogy (X-ray powder diffraction analysis, scanning electron microscope imaging, confocal Raman microscopy, electron microprobe analysis) and isotope composition ($\delta^{18}O$ and $\delta^{13}C$) of non-skeletal carbonate minerals in a Lake Van sedimentary profile spanning the last ca. 150 kyr. Carbonate phases present in the sediment include aragonite, low-Mg calcite, and calcian dolomite. Dolomite forms as an early diagenetic phase and occurs episodically in high concentrations driving the bulk isotope record towards the higher dolomite $\delta^{18}O$ and varying $\delta^{13}C$ values. Aragonite and low-Mg calcite precipitate in the surface water and are present in the sediments in varying amounts (relative aragonite to calcite content for dolomite-poor samples Ar/(Ar + Cc) of 93 to 41 wt%). In an attempt to explain this variation, we revised a precipitation model based on annually laminated sediments containing both aragonite and calcite spatially separated in light and dark coloured laminae, respectively. According to our model, spring calcite precipitation, under close-to-freshwater conditions, is followed by evapoconcentration-driven aragonite precipitation in late summer. The precipitation of these carbonate polymorphs from chemically differing surface waters (i.e. freshwater-influenced and evapoconcentrated) leads to distinctly different oxygen and carbon isotope signatures between sedimentary penecontemporaneous aragonite and calcite. The $\delta^{18}O$ and $\delta^{13}C$ values of aragonite relative to calcite are significantly higher by several per mille than inferred from aragonite-calcite fractionation factors alone, suggesting that the generalised assumption of sedimentary coeval calcite and aragonite precipitating from water with the same isotopic composition is flawed. The here proposed revised hydrologically-separated carbonate precipitation model is not only taking (i) differences in the isotopic fractionation between carbonate minerals into account, but also (ii) considering the hydrological conditions and the processes favouring the precipitation of a given mineral and ultimately controlling its isotopic composition. If mixed mineralogies are present, this mineralogy-specific approach has the potential of refining environmental reconstructions and reconciling apparently equivocal interpretations of different proxy records.

1. Introduction

In continental palaeoclimatology, oxygen and carbon isotope ($\delta^{18}O$ and $\delta^{13}C$) analysis of lake carbonates is a routinely applied technique to investigate, among others, changes in temperature, the meteoric precipitation/evaporation ratio (P/E), productivity, and the lakes hydrological state (i.e. hydrologically open versus closed; see reviews by Talbot, 1990; Leng and Marshall, 2004; Deocampo, 2010; Bernasconi and McKenzie, 2013 and references therein). Despite its frequently inhomogeneous nature, bulk carbonate remains the most common target material for isotope analysis. Compared to inorganic carbonates, biogenic carbonates are often only a minor component of lacustrine sediments, with little impact on the bulk sediment geochemistry. In absence of detrital (Leng et al., 2010; Mangili et al., 2010) or diagenetic components (Lacey et al., 2015; McCormack et al., 2018), the bulk carbonate is mainly represented by inorganic carbonates precipitated within

* Corresponding author.
E-mail address: jeremy.mccormack@rub.de (J. McCormack).

https://doi.org/10.1016/j.chemgeo.2019.03.014
Received 15 June 2018; Received in revised form 4 March 2019; Accepted 10 March 2019
Available online 14 March 2019

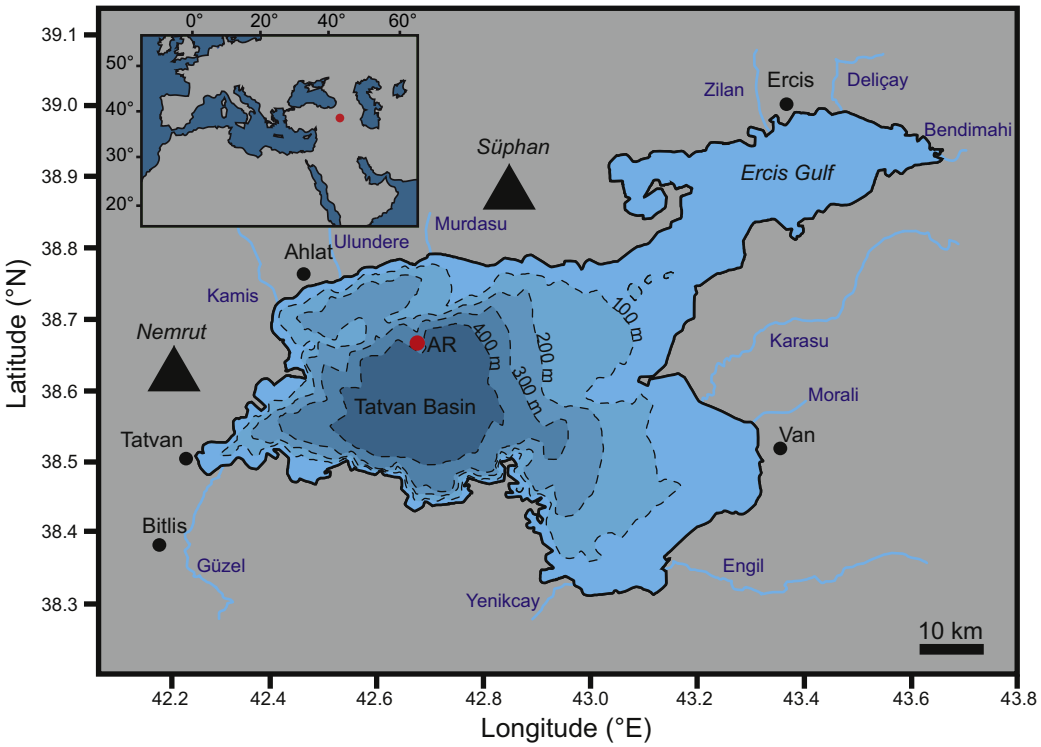

Fig. 1. Location and bathymetry of Lake Van (Turkey) with the position of the ICDP Ahlat Ridge drill site (red dot) (modified after Kaden et al., 2010; Stockhecke et al., 2012; Pickarski et al., 2015a). The locations of adjacent major cities are indicated by black dots and active volcanoes by black triangles. (For interpretation of the references to colour in this figure legend, the reader is referred to the web version of this article.)

the water column. However, within a given layer, lake sediments often contain more than one inorganic carbonate phase (e.g. aragonite, low- and high-magnesium calcite, dolomite, siderite) not all of which necessarily precipitate under the same hydrochemical conditions (water column versus authigenic precipitation in the pore space) or at the same time (seasonality).

Unless recognised, the presence of diagenetic carbonates (e.g. dolomite, siderite) coexisting with primary surface water precipitates (e.g. aragonite, calcite) can compromise interpretations of lacustrine $\delta^{18}O$ and $\delta^{13}C$ signals obtained from bulk material (Lacey et al., 2015; McCormack et al., 2018). The isotopic composition of the diagenetic phases can vary from the intended target water column precipitates, depending on the timing of diagenetic precipitation and the isotopic composition and temperature of the porewater compared to the surface water. Still, even in the absence of early diagenetic carbonate minerals, aragonite and calcite, both calcium carbonate ($CaCO_3$) polymorphs are commonly believed to form simultaneously within the epilimnion, particularly in many closed lakes (e.g.; Yu and Kelts, 2002; Dean et al., 2015), and are often present within the same sedimentary layer or interval. Whether the precipitation of aragonite or calcite is favoured is dependent on various hydrochemical conditions such as the lake water Mg/Ca ratio, temperature and the saturation state of $CaCO_3$ in the aqueous solution (e.g. Müller et al., 1972; Burton and Walter, 1987; González and Lohmann, 1988; Fernández-Diaz et al., 1996; Morse et al., 1997; De Choudens-Sánchez and González, 2009). The relative aragonite to calcite content in sediment profiles of lakes is therefore commonly interpreted in terms of changing hydrochemical conditions. The environmental changes (e.g. P/E ratio) driving these hydrochemical conditions (e.g. Mg/Ca ratio) are likely to impact also the $\delta^{18}O$ of the lake water ($\delta^{18}O_{lake}$) and the $\delta^{13}C$ of dissolved inorganic carbon (DIC; $\delta^{13}C_{DIC}$). In closed lakes, for example, the oxygen isotopic composition of the lake water is particularly sensitive to climate induced changes in the P/E ratio with $\delta^{18}O_{lake}$ values varying up to several per mille with shifting P/E ratios (Leng and Marshall, 2004). Subsequently, an increasing trend in carbonate $\delta^{18}O_{bulk}$ values from closed lakes is predominantly interpreted as lowering P/E ratios, while decreasing $\delta^{18}O$ values indicate rising P/E ratios.

If $CaCO_3$ polymorph precipitation varies within an annual cycle or hydrochemically distinct water masses (e.g. at varying water column depths), the isotopic composition of the precipitating polymorphs will also likely vary. This might lead to different isotopic signals in sedimentary coeval $CaCO_3$ polymorphs. Only a handful of studies investigated detrital or diagenetic carbonates separately from the bulk material or their influence on the intended target carbonate phase precipitating from the water column (e.g. Leng et al., 2010; Mangili et al., 2010; Lacey et al., 2015; McCormack et al., 2018). Similarly, few studies describe different mechanisms behind variations in aragonite/calcite ratios of lacustrine sedimentary profiles (e.g. Murphy et al., 2014; Roeser et al., 2016). Hitherto no study focused on the isotopic influence of individual $CaCO_3$ polymorphs on the bulk isotopic composition of lacustrine mixed aragonite-calcite material beyond the differences in aragonite-calcite fractionation factors.

Bulk sediments from alkaline waters of Lake Van in Eastern Anatolia, Turkey, represent an excellent case example of an apparently inconsistent oxygen isotope record (Kwiecien et al., 2014) with a complex carbonate mineralogy (Landmann et al., 1996; Çağatay et al., 2014; McCormack et al., 2018). Among the ambiguities of the $\delta^{18}O$ bulk record ($\delta^{18}O_{bulk}$) from Lake Van are similar mean $\delta^{18}O_{bulk}$ values for climatically distinct periods for which non-carbonate proxy records document significant hydrological changes (Kwiecien et al., 2014). Also, although seasonal carbonate precipitation events (whitings) are clearly documented (Kempe and Kazmierczak, 2003; Stockhecke et al., 2012) and Holocene sediments are annually laminated, there is no coherent model for carbonate precipitation in the lake (e.g. Degens et al., 1984; Landmann et al., 1996; Stockhecke et al., 2012). Existing hydrochemical data for Lake Van water (Kempe et al., 1990; Lemcke, 1996; Reimer et al., 2009) and $CaCO_3$ mineralogy sediment trap data (Stockhecke et al., 2012) are scarce and not seasonally-resolved, which hampers water-carbonate chemistry calibration attempts. This study aims at reconciling contradicting reports on Lake Van carbonate precipitates and disentangling its problematic carbonate bulk stable isotope record. The target material stems from sediment cores recovered by the International Continental Scientific Drilling Program (ICDP) at the Ahlat Ridge (AR) site, dating back approximately 147 kyr. Here we

combine mineralogical and stable isotope analyses to investigate the nature, timing, controls and site of carbonate precipitation in Lake Van. Our overreaching goal is to refine the understanding of lacustrine carbonate-based palaeoenvironmental proxies. The isotopic composition of an individual polymorph is inherently related to the mechanisms favouring its precipitation. Consequently, the understanding of these mechanisms is essential for an accurate interpretation of the isotopic composition of mixed bulk carbonates records.

2. Limnological setting

Lake Van is a deep (460 m), terminal alkaline lake situated on a high plateau in Eastern Anatolia, Turkey (Fig. 1). Today's lake level is at an altitude of 1648 m above sea level (a.s.l.). Lake Van is bordered to the south by metamorphic rocks of the Bitlis-Pötürge Massif (Mutlu et al., 2012) and in the eastern part by Tertiary and Quaternary sandstones, conglomerates and carbonates (Stockhecke et al., 2014a). Pliocene and Quaternary volcanics dominate the west, north and northeast of Lake Van (Degens et al., 1984). The volcanic hinterland of the lake in combination with high evaporation rates is directly responsible for the lake Na-CO_3-Cl chemistry, characterised by nearly equal shares of sodium carbonate and sodium chloride (Kempe et al., 1991; Litt et al., 2012). The lakes total alkalinity reaches approximately 151 mmol l^{-1}, salinity approximately 22 g kg^{-1} and pH 9.7–9.8 (Kempe et al., 1991; Reimer et al., 2009; Litt et al., 2012). The concentrations of Mg^{2+} is low but Ca^{2+} is strongly depleted with respect to other ions, resulting in an Mg/Ca ratio between 42 and 52 (Kempe et al., 1991; Reimer et al., 2009). It is the low Ca^{2+} ion activity that, despite a carbonate supersaturation throughout the water-column (Lemcke, 1996; Reimer et al., 2009) limits carbonate precipitation in Lake Van. Total alkalinity and concentration of most ions including Cl^-, Na^+, SO_4^{2-}, K^+ and Mg^{2+} increase with depth towards the halocline. Due to the influence of Ca^{2+}-rich spring freshwater input, Ca^{2+} concentrations and $CaCO_3$ saturation peak in the epilimnion (during spring and early summer) and decrease abruptly below the epilimnion (Reimer et al., 2009). Lemcke (1996) and Reimer et al. (2009) suggested a near quantitative precipitation of annual riverine Ca^{2+} inflow as $CaCO_3$, based on an estimated annual Ca river influx (~23 g m^{-2} a^{-1}) and calculated mean Ca sediment deposition rates (~20 g m^{-2} a^{-1}). Recent carbonate precipitation within Lake Van's surfacial water masses (epilimnion or possibly an epilimnion-hypolimnion mixing zone) takes place in the form of two seasonally separated types of whitings (Kempe and Kazmierczak, 2003): (i) spring runoff resulting from increased meteoric precipitation and meltwater delivers Ca^{2+} ions, leading to carbonate precipitation within river plumes (Landmann et al., 1996; Kempe and Kazmierczak, 2003; Stockhecke et al., 2012). (ii) in the hot and dry late summers, a second phase of carbonate precipitation takes place coinciding with an annual minimum of the lake level (Kaden et al., 2010), likely coupled to evaporative supersaturation in a thermally stratified surface layer (upper ~10 m; Landmann and Kempe, 2002; Kempe and Kazmierczak, 2003; Stockhecke et al., 2012). In winter, carbonate precipitation ceases, and reduced surface-water temperatures and stronger winds result in mixing of the uppermost 70 m of the water column, whereas the deep water remains suboxic (Kaden et al., 2010; Huguet et al., 2011; Stockhecke et al., 2012). Significant dissolution of carbonate minerals within the water column or the sediment is not expected in modern Lake Van, as water column Ca^{2+} concentrations remain low and $CaCO_3$ remains highly supersaturated (Reimer et al., 2009). Modern $\delta^{18}O$ values for river water entering Lake Van were estimated to lie between −11.5 and –10.1‰ VSMOW (Faber, 1978). Only early summer $\delta^{18}O$ values are documented for the lake's surface water, and are between −0.4 and 1‰ VSMOW (Kempe et al., 1990; Jasechko et al., 2013).

With a particle settling time of significantly < 3 months, modern seasonal fluctuations of surface water particle formation and inflow are recorded in deep sediments (Stockhecke et al., 2012). The deposition of finely laminated sediments (varves) during interglacials and interstadials suggests the persistence of conditions similar to modern ones during these intervals. The finely laminated sediments were deposited under suboxic/anoxic conditions with commonly higher total organic carbon (TOC), arboreal pollen and carbonate content all resulting from increased moisture availability and a rising/high lake level (Kwiecien et al., 2014; Stockhecke et al., 2014a; Pickarski et al., 2015a, 2015b). Increased freshwater input enhanced density gradients and reduced advective water-column mixing, prompting an upward migration of the oxic-anoxic boundary and the subsequent preservation of varves (Kaden et al., 2010; Stockhecke et al., 2014a).

3. Isotope geochemistry and mineralogy of Lake Van carbonates – state of the art

Earlier interpretations of Lake Van's $\delta^{18}O$ bulk records ($\delta^{18}O_{bulk}$) spanning about 14.7 kyr appeared to be consistent with other proxies (Landmann et al., 1996; Lemcke and Sturm, 1997; Wick et al., 2003). The Younger Dryas (YD), a cooling period, that interrupted the warming into the Holocene over most of the Northern Hemisphere, is represented by a shift towards higher values in the Lake Van $\delta^{18}O_{bulk}$ record (Lemcke and Sturm, 1997). The higher YD $\delta^{18}O_{bulk}$ values explained in terms of intensified aridity, were supported by Lake Van's arboreal pollen data also documenting arid conditions during the time period (Wick et al., 2003). However, beyond 14.7 kyr, the comparison of $\delta^{18}O_{bulk}$ data is clearly at odds with all other proxy records (Kwiecien et al., 2014). Higher $\delta^{18}O_{bulk}$ values appear in both cold and arid periods such as the YD and in warm and wet periods such as the Last Interglacial (MIS 5e) challenging the integrity of previous explanations of the $\delta^{18}O_{bulk}$ record. Inconsistent accounts on the nature of inorganic carbonates add yet another dimension to the problem. Mineralogical investigations performed on both sediment traps and core material have reported inorganic $CaCO_3$ epilimnion precipitates solely as either aragonite (e.g. Müller et al., 1972; Irion, 1973; Degens et al., 1984), calcite (Stockhecke et al., 2012), or both (Landmann et al., 1996; Lemcke, 1996; Lemcke and Sturm, 1997; Reimer et al., 2009; Çağatay et al., 2014) (Table 1). Although dolomite was documented in previous studies (Khoo et al., 1978; Degens et al., 1984; Landmann et al., 1996) only a recent systematic and detailed approach revealed its diagenetic origin (McCormack et al., 2018).

The presence of inorganically precipitated low-magnesium calcite in Lake Van's surface water is unexpected and still not adequately resolved. The Mg/Ca ratio of 42–52 in Lake Van (Reimer et al., 2009) is normally considered too high for calcite precipitation (Müller et al., 1972; De Choudens-Sánchez and González, 2009). A possible explanation was proposed by Degens et al. (1984) who noticed a spatial separation between calcite and aragonite within the varved sediments of Lake Van, with calcite dominating the dark laminae and aragonite the light laminae. These authors explained the presence of calcite in an environment seemingly unfavourable for its formation as a diagenetic product of SO_4^{2-} reduction in organic-rich layers. A diagenetic origin of calcite, however, contrasts with subsequent studies documenting calcite in sediment traps indicating its nucleation within the water column (Landmann et al., 1996; Stockhecke et al., 2012). Landmann et al. (1996) and Lemcke (1996) proposed that, due to the lower Mg/Ca ratio of the river water, calcite may be able to precipitate within the well-documented river plume whitings. River plumes can extend far into the basin (Stockhecke et al., 2012) and calcite may be transported even further due to its small crystal size (Landmann et al., 1996). The documented river plume whitings are in line with saturation index calculations by Lemcke (1996) demonstrating that modern calcite precipitation is possible within Ca-rich river plumes even when the freshwater mixes with far < 20% of Lake Van's water. Neither the calcite precipitation hypothesis itself, formulated to account for the spatial and/or temporal variation of calcite and aragonite precipitation, nor its implications for stable isotope analyses of samples containing both polymorphs (i.e. bulk samples) were further developed.

Table 1
Compilation of selected literature reporting the mineralogy of Lake Van carbonates, highlighting the inconsistency in observed mineral phases and proposed precipitation mechanisms, n.d. indicates that either the material, site or mechanism of precipitation were not specifically discussed.

Publication	Sample material and site	Reported carbonate phase	Proposed site of precipitation	Suggested precipitation mechanism
Müller et al. (1972)	n.d.	Aragonite	Water column	Within river plume whitings due to Ca^{2+} supply
Irion (1973)	Sediment cores (unknown depth and location)	Aragonite	Water column	Within river plume whitings due to Ca^{2+} supply
		Calcite	n.d.	shown in an XRD-diagram but mentioned neither in a table nor the text
Khoo et al. 1978	sediment cores from varying water depths (17–400 m)	Calcite	Sediment	Diagenetic, linked to SO_4^{2-} reduction
		Aragonite	Water column	Within river plume whitings due to Ca^{2+} supply, perhaps via a monohydrocalcite precursor
		Dolomite	Sediment or water column	Under a low lake level with particularly a high Mg/Ca ratio
Degens et al. (1984)	Review paper re-evaluating previous interpretations	Calcite	Sediment	Diagenetic, linked to SO_4^{2-} reduction
		Aragonite	Water column	Within river plume whitings due to Ca^{2+} supply
		Dolomite	Sediment, under subaerial exposure	Evaporative supersaturation during periods of increased aridity
Landmann et al. (1996)	Sediment cores from varying water depths (115–446 m), sediment trap in the Tatvan Basin (water depth 120 and 400 m)	Low-Mg calcite	Water column	Within river plume whitings due to Ca^{2+} supply
		Aragonite	Water column	Increased Ca^{2+} concentration resulting from summer evaporation
		Stoichiometric dolomite	Water column or detrital	n.d.
		Calcian dolomite, termed "protodolomite" and magnesite	n.d.	Evaporative supersaturation during periods of increased aridity
Lemcke (1996); Lemcke and Sturm (1997)	Sediment cores from varying water depths (115–446 m), sediment trap in the Tatvan Basin (water depth 120 and 400 m)	Aragonite	Water column	Increased Ca^{2+} concentration resulting from summer evaporation
		Low-Mg calcite	Water column	Within river plume whitings due to Ca^{2+} supply
		Dolomite, high-Mg calcite and Ca-magnesite	n.d.	Evaporative supersaturation during periods of increased aridity
Stockhecke et al. (2012)	Sediment trap in the Tatvan Basin (water depth between 35 and 440 m)	Calcite	Water column	Within river plume whitings due to Ca^{2+} supply and photosynthetic CO_2 removal/evapoconcentration
Çağatay et al. (2014)	Sediment core from the Northern Basin (water depth of 245 m)	Calcite	Water column	Associated with lower salinities and less evaporative conditions
		Aragonite	Water column	Associated with higher salinities and evaporative conditions
		Dolomite	n.d.	Evaporative supersaturation during periods of increased aridity
McCormack et al. (2018)	Sediment core from the Ahlat Ridge (water depth of 360 m)	Low-Mg calcite	Water column	n.d.
		Aragonite	Water column	n.d.
		Calcian dolomite	Sediment	Likely microbially-mediated, related to environmental stress following a lake level fall and a re-ventilation of the lake bottom
		Possible stoichiometric dolomite	Possibly detrital	Possibly detrital

4. Material and methods

4.1.1. Material

The sediments from Lake Van studied here were recovered in the summer of 2010 in the frame of the ICDP PALEOVAN project (Litt et al., 2012; Litt and Anselmetti, 2014). For this study, we resampled the Ahlat Ridge (Fig. 1) composite profile and off-section material. Visual correlation based on high-resolution images allowed assigning composite profile depth and age (after Stockhecke et al., 2014b) to off-sections samples. The lithological description was performed on high-resolution composite profile images based on the lithotypes and their genetic interpretation, published in detail in Stockhecke et al. (2014a). The data presented here represent the uppermost 67 m of the composite profile (55 m when excluding event deposits, i.e. no-event composite profile) corresponding to a duration of ca. 147 kyr.

4.1.2. Sample preparation

A total of 216 samples were collected, with a single sample resolution of 2 cm (mean temporal resolution ca. 54 years). Event deposits such as tephra and graded layers were avoided during sampling. To separate inorganic from biogenic carbonates (ostracod valves) the samples were wet-sieved with distilled water through a succession of sieves with mesh sizes of 250, 125, and 63 μm. The fine fraction < 63 μm was collected in a glass container and after settling decanted through filter paper and air-dried at room temperature. An aliquot of each dried fine fraction samples was homogenised in an agate mortar for XRD and isotope analysis. For SEM analysis not homogenised bulk samples were used as well as bulk samples that were neither sieved nor homogenised, for which the only processing involved oven-drying (50 °C).

To investigate whether calcite and aragonite can be linked to specific laminae as suggested by Degens et al. (1984) we have analysed an exemplary thin section of varved Holocene sediment by means of confocal Raman microscopy and electron microprobe analysis. The respective thin section (from a core depth of approximately 20–23 cm) was produced from a short (approximately 110 cm) sediment core Van07-06 taken in 2007 from the Ahlat Ridge (Stockhecke, 2008), corresponding to an interval between ca. 144–204 yr BP.

4.2. Scanning electron microscopy and X-ray powder diffraction analysis

SEM imaging was performed to document the carbonate crystal morphologies. Samples were coated with a thin gold layer and analysed using a LEO/Zeiss Gemini 1530 as well as a Gemini 2 – Merlin, both operating with an acceleration voltage of 20 kV. Energy-dispersive X-ray spectroscopy in combination with the AZTec software package from OXFORD Instruments were used to differentiate between Mg-bearing carbonates (dolomite) and Ca-carbonates.

The aim of X-ray powder diffraction analysis was a semi-quantitative analysis of the relative abundance (weight percentage) of different carbonate minerals. Analyses were performed on a Bragg-Brentano diffractometer (PANalytical's Empyrean) equipped with a PIXcel1D detector. Samples were analysed using Cu K_α radiation, applying a tube voltage and current of 45 kV and 40 mA respectively. Scanning was carried out from 4 to 65° 2Theta with a step size of 0.0131° and a counting time of 3 s per step. Furthermore, operating conditions included fixed 0.25° divergent and 0.5° antiscatter slits in the incident beam path, incident and diffracted beam 0.04 rad soller slits and a 7.5 mm high antiscatter slit together with a Ni Filter in the diffracted beam optics.

Mineral identification and estimates of the relative proportions of carbonate phases (aragonite, calcite, and dolomite) were performed with the PANalytical X'Pert HighScore Plus software and based on mineral Relative Intensity Ratios (RIR). A fully quantitative mineralogical analysis is problematic here due to the complexity of the mineral assemblage. Consequently, as only relative proportions of the carbonate mineral phases are of relevance for this study the use of RIR calibration factors is sufficient enough in this case (Snyder, 1992).

$MgCO_3$ in calcite and dolomite in mole percentage was semi-quantitatively established following Goldsmith et al. (1961) and using the equation of Lumsden (1979):

$$NCaCO_3 = 333.33\ d – 911.99$$

where $NCaCO_3$ is the mol% $CaCO_3$ in the calcite/dolomite lattice and d is the d spacing in Å of the 104 peak. The position of calcite and dolomite 104 reflections were obtained using quartz as an internal standard.

4.3. Confocal Raman microscopy

Identification of the mineral phases within the sample was performed using a WITec alpha 300 R Confocal Raman Microscope (CRM) equipped with an ultra-high throughput spectrometer (UHTS 300). The spectrometer (grating used: 600/mm, and 500 nm blaze) was connected to the microscope with an optical fibre having a 50 μm pinhole). Excitation wavelength was 488 nm (diode Laser) and the objective used a Nikon MPlan Fluo 100× with a numerical aperture (N.A.) of 0.9. Initially CRM measurements where performed in order to test the possibility to perform the imaging of larger sample areas to visualise the mineral distribution in 2D (as described in e.g. Nehrke and Nouet, 2011). In the context of these analyses, it turned out that due to the high background fluorescence of the samples (tested with excitation wavelength of 488, 532, and 785 nm), mapping of larger sample areas was not possible. However, using an objective with a high N.A. (0.9) and an integration of 10 spectra measured for 2 s showed that spot measurements within dedicated areas allow for a reliable identification of single mineral grains. Due to the nature of the sample the focal plane changes slightly for every mineral grain measured by CRM. Therefore it was necessary to optimize the signal to noise ratio in the Raman spectra for every spectra recorded by carefully adjusting the instrument to the right focal plane. This time consuming process made it impossible to perform an automated CRM imaging over larger areas of the sample.

4.4. Electron microprobe analysis

X-ray element distribution maps were acquired with a Cameca SXFiveFE field emission electron microprobe at the Ruhr-University Bochum. The microprobe is equipped with five wavelength-dispersive spectrometers (WDS) as well as an energy-dispersive system (EDS) with a silicon drift detector. Measurements were performed on a gold-coated thin section using 15 kV acceleration voltage and 80 nA probe current. The X-ray lines of Sr, Ca, P, Na and Si were measured using WDS, whereas Mg, Al, K and Fe were measured with the EDS. An overview image (Fig. 2c–f) was measured using 65 ms dwell time and a step width of 1.0 μm, a more detailed image (Fig. 2h–i) with 75 ms and 0.5 μm step width.

4.5. Carbon and oxygen isotope analysis

Carbon and oxygen isotope analyses were performed in continuous flow mode following the procedure described in Breitenbach and Bernasconi (2011) using a GasBench II coupled to a ThermoFinnigan MAT 253 mass spectrometer at the Ruhr-University Bochum. Due to the very low organic content (Stockhecke et al., 2014a), no pre-treatment to remove organics was performed. Between 90 and 300 μg (in some cases up to 1000 μg) sample powder (homogenised fine fraction), depending on the carbonate content was weighed into borosilicate glass vials and oven-dried at 104 °C overnight. Samples were run at 70 °C for 1 h together with international standards NBS19, IAEA603, CO8 and ETH-1 (ISO-A, Meckler et al., 2014). All results are reported with

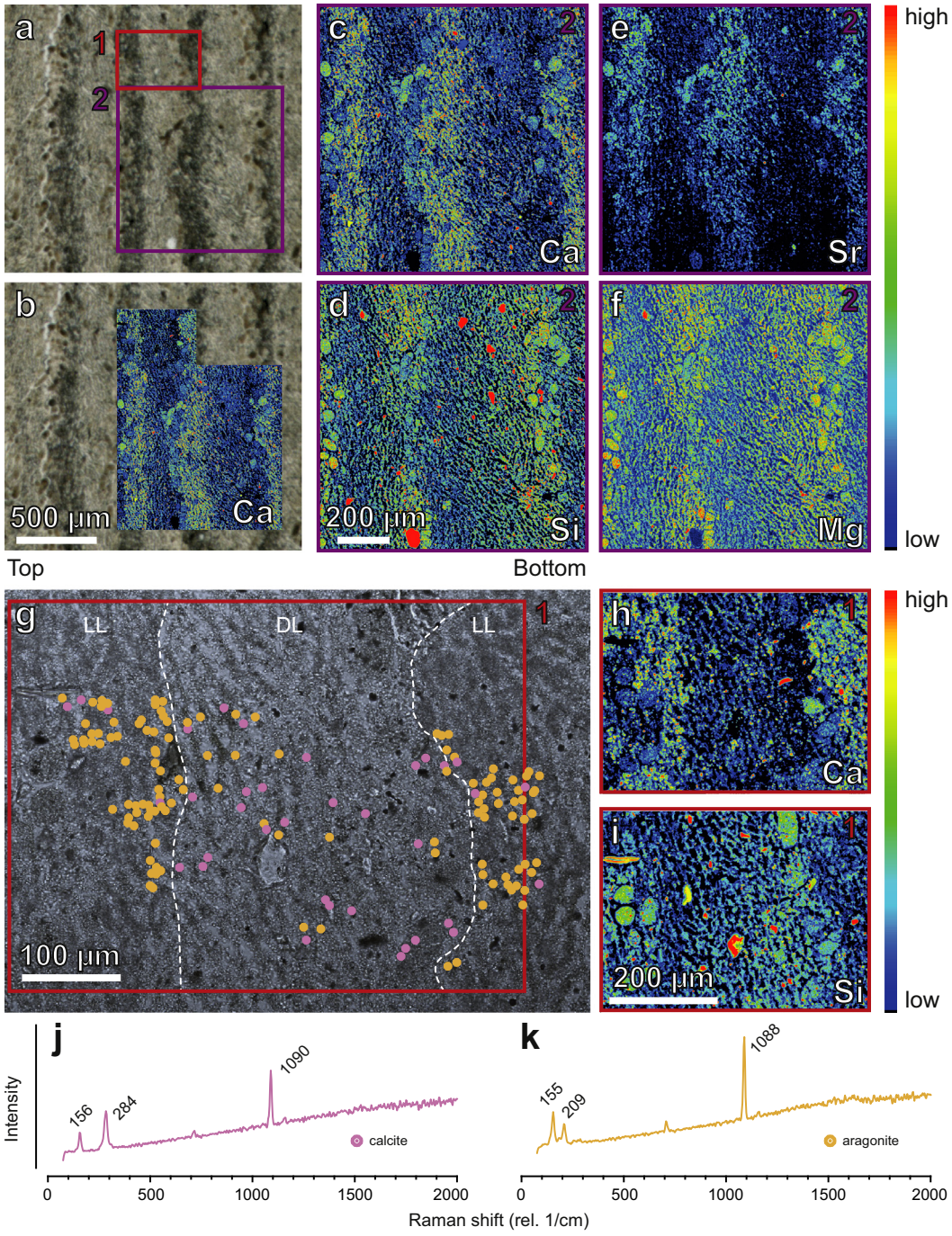

Fig. 2. Electron microscope and Confocal Raman microscopy results from Holocene varved sediments. The overview images presented here (a, b, g) were taken under transmitted light, resulting in a reversal of the colouring, i.e., light laminae (LL) appear dark under transmitted light and vice versa. a) Overview of light and dark laminae (DL) and area of depicted microprobe and CRM measurements as red coloured box 1 (b, g–i) and yellow coloured box 2 (b, c–f). b) Ca distribution map. c–f) Detailed Ca (c), Si (d), Sr (e) and Mg (f) distribution maps from area 2 depicted in a). Light laminae are characterised by highest Ca and Sr concentrations, while dark laminae are enriched in Si and Mg. g) CRM spot results identifying carbonate minerals within a dedicated area (box 1). Purple dots represent calcite grains (more abundant in the dark laminae) and orange dots aragonite grains (dominating in the light laminae). h,i) Detailed Ca (h) and Si (i) distribution maps for area 1. j,k) Examples of calcite (purple) and aragonite (orange) Raman spectra used to identify the carbonate grains as depicted in g). Boundaries used for laminae separation are indicated in (g). (For interpretation of the references to colour in this figure legend, the reader is referred to the web version of this article.)

respect to the Vienna Pee Dee Belemnite (VPDB) standard, unless otherwise indicated. The external standard deviation for oxygen is < 0.08‰, and for carbon < 0.07‰. The isotopic composition of isolated dolomite and details regarding sample preparation and measurement are reported in McCormack et al. (2018).

5. Results

5.1. Mineralogy

5.1.1. Scanning electron microscopy and X-ray powder diffraction analysis

The main mineral fraction, identified by XRD analyses, are carbonates minerals, represented in nearly all samples by aragonite, calcite

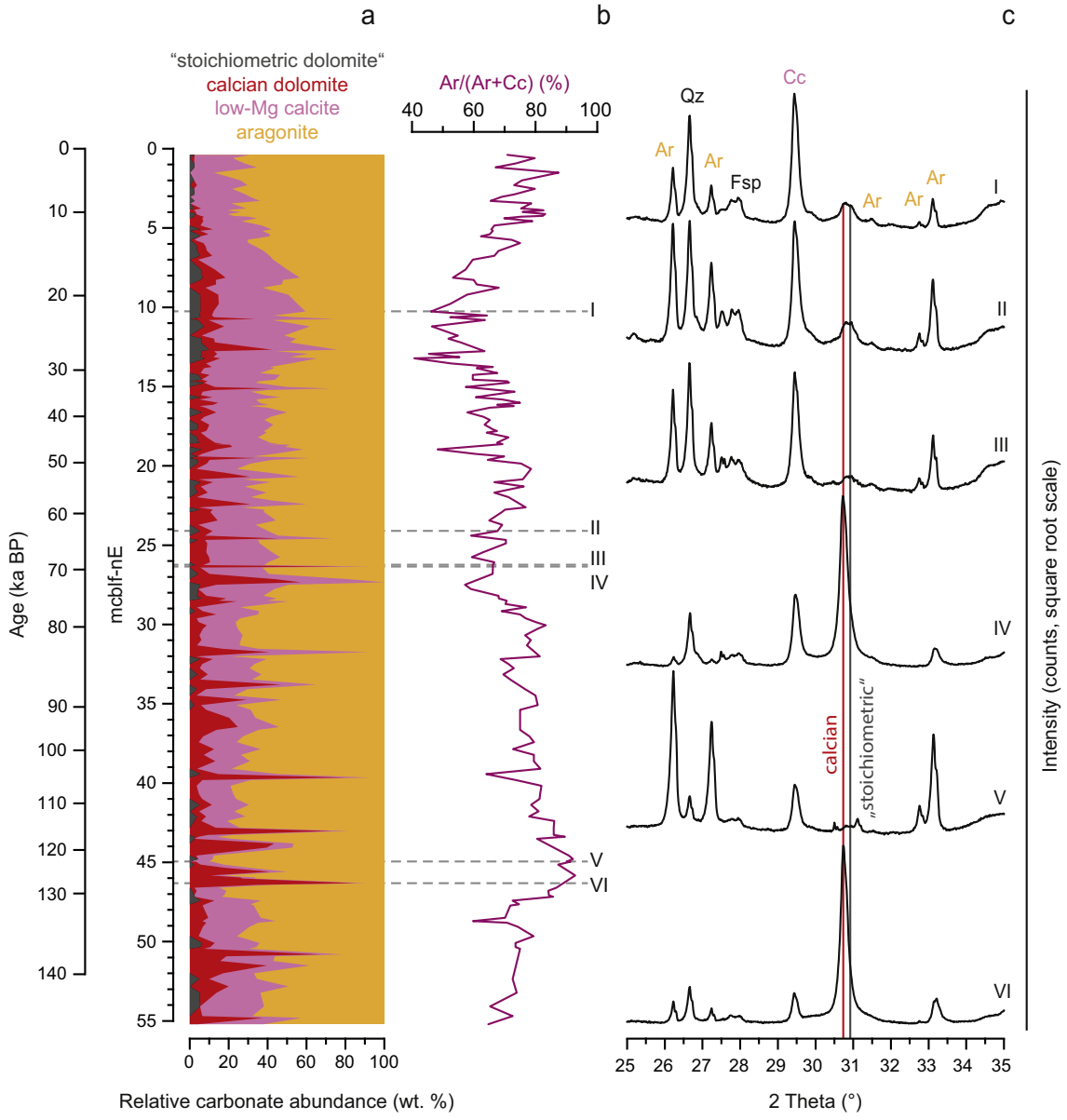

Fig. 3. Changes in the relative carbonate abundance with depth in metre composite below lake floor – no-event scale (mcblf-nE) and age (ka BP). a) Relative distribution of carbonate minerals. b) Relative aragonite content for dolomite poor samples (< 15 wt% dolomite) expressed by an aragonite/non-dolomite content Ar / (Ar + Cc) in weight %. c) XRD pattern variability of selected samples (I–VII) with major mineral peaks for aragonite (Ar), quartz (Qz), feldspar (Fsp), calcite (Cc), calcian, non-stoichiometric dolomite and a possible stoichiometric dolomite.

and calcian dolomite. Generally, aragonite is the dominant carbonate species (Fig. 3a). Non-carbonate minerals include quartz, feldspar, and clay minerals. All calcites identified here are low-magnesium calcite with d_{104}-values varying between 3.027 and 3.033 Å, indicating 1 to 3 mol% $MgCO_3$. Calcian dolomite in Lake Van sediments has been recently described in detail by McCormack et al. (2018). The contribution of calcian dolomite (53 to 59 mol% $CaCO_3$) to the relative carbonate content ranges between below detection limit, to being the dominant carbonate mineral with > 40 to 85% of the relative carbonate fraction (Fig. 3a). The concentration of an additional mineral phase with d_{104}-values of 2.884 to 2.892 Å indicative of stoichiometric to near-stoichiometric dolomite remains at background levels near XRD detection limit.

As calcian dolomite forms diagenetically, likely by replacing primary carbonates (McCormack et al., 2018), samples with high dolomite content (> 15%) were not considered here for assessing variations in calcium carbonate formation within the water column. Aragonite accumulation and/or preservation in the sediments can be expressed by an aragonite/non-dolomite carbonate content (Ar / (Ar + Cc) multiplied with 100 and given in weight %) representing the concentration of aragonite (Ar) relative to calcite (Cc) in dolomite poor samples. In the material studied here, the (Ar / (Ar + Cc) varies between ~41 and 93% (Fig. 3 b). In general, the highest (Ar / (Ar + Cc) (81–93%) are featured during MIS 5e. High, but more variable than during MIS 5e (Ar / (Ar + Cc) values are also reached in the Holocene (65–85%). Lowest aragonite concentrations in samples with low dolomite content are recorded during MIS 2 and 3 (41–79%) with mean values of 63%.

Aragonite crystals are of uniform size and form elongated needles reaching between ~2 and 8 µm in length. They occur as individual needle-like crystals or bundles (Fig. 4a, b). Calcite crystals also have a homogenous size distribution, are euhedral with variable morphology (equant and prismatic), reaching dimensions of between ~2 and 10 µm (Fig. 4c, d). Dolomite crystals display complex growth features of interpenetrating dolomite rhombs (Fig. 4e, f), are more variable in size

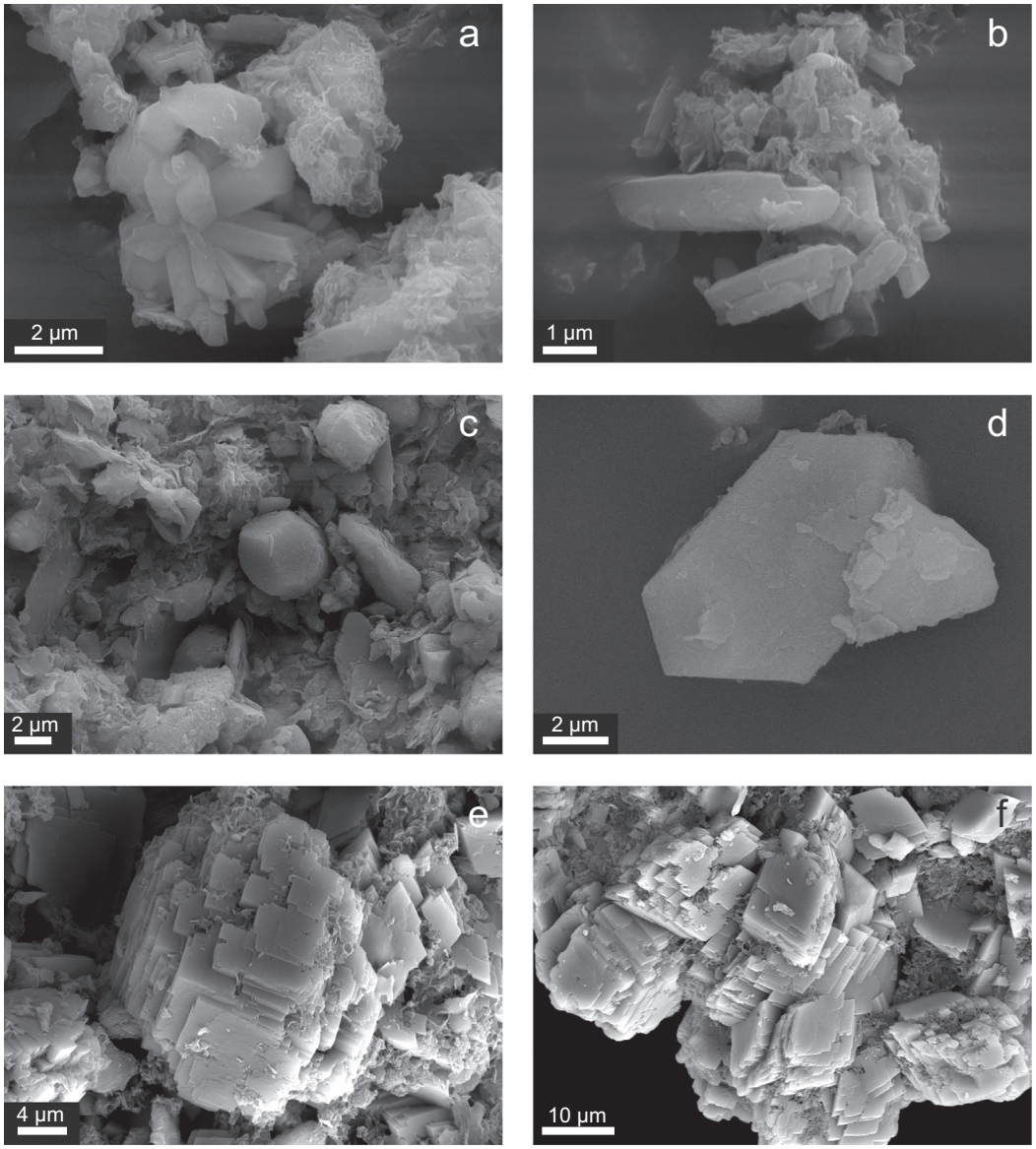

Fig. 4. Scanning electron microscope images of selected Lake Van carbonate minerals. a,b) Aragonite needles from 53.692 mcblf. c,d) Calcite crystals from 12.954 mcbfl. e,f) Dolomite crystals from 56.824 mcblf.

~2–40 µm, and typically larger than aragonite and calcite crystals.

5.1.2. Confocal Raman microscopy and electron microprobe analysis

Confocal Raman microscopy (CRM) and electron microscopy were performed on Holocene varves, which in Lake Van consist of submillimetre scale alternating dark and light laminae (Fig. 2a). Note that varve images presented here (Fig. 2a, b, g) were taken under transmitted light, which results in a reversal of the colouring, i.e., light laminae appear dark under transmitted light and vice versa.

Out of the 323 carbonate grains analysed by CRM, 236 were identified as aragonite and 87 as calcite (e.g. Fig. 2j, k). The highest concentration of measurable carbonate minerals was found within the light (dark in transmitted light) varve laminae (Fig. 2g). Although the identification of distinct boundaries between the dark and light laminae is challenging, tentative calculations of the aragonite and calcite distribution based on CRM analyses suggest that 85% of the carbonate within the light laminae has an aragonitic mineralogy (15% calcite), whereas in the dark laminae only 32% of the carbonates are identified as aragonite (68% calcite; Fig. 2g). A comparison with electron microprobe element maps highlights that light laminae are Ca- and Sr-enriched and composed mainly of carbonate minerals (mainly aragonite) (Fig. 2 b, c, e, h), while the dark laminae contain mostly Si-Mg minerals (Fig. 2d, f, i). Consequently, aragonite is the dominant polymorph in the carbonaceous light laminae, while calcite is more frequent in the siliciclastic dark laminae.

5.2. Isotopic composition of inorganic carbonates

The $\delta^{18}O$ and $\delta^{13}C$ values of the sieved fine fraction (< 63 µm) are a compositional mixture of the individual isotopic values of aragonite, calcite, and dolomite ($\delta^{18}O_{Ar+Cc+D}$ and $\delta^{13}C_{Ar+Cc+D}$). $\delta^{18}O_{Ar+Cc+D}$ varies between −4.5 and + 4.7‰ and $\delta^{13}C_{Ar+Cc+D}$ values vary between +1.2 and + 7.3‰. The signature of $\delta^{18}O_{Ar+Cc+D}$ (Fig. 5b) is similar to the published $\delta^{18}O_{bulk}$ record (Fig. 5a) documented in Kwiecien et al. (2014) and featuring the same events (e.g. positive YD excursion).

The isotopic composition of dolomite-poor samples (< 15%; $\delta^{18}O_{Ar+Cc}$ and $\delta^{13}C_{Ar+Cc}$) shows generally the same behaviour as the $\delta^{18}O_{bulk}$ (Fig. 5a, b). Highest $\delta^{18}O$ values are reached during the Last Interglacial, the YD, and during the late Holocene. Notably, samples

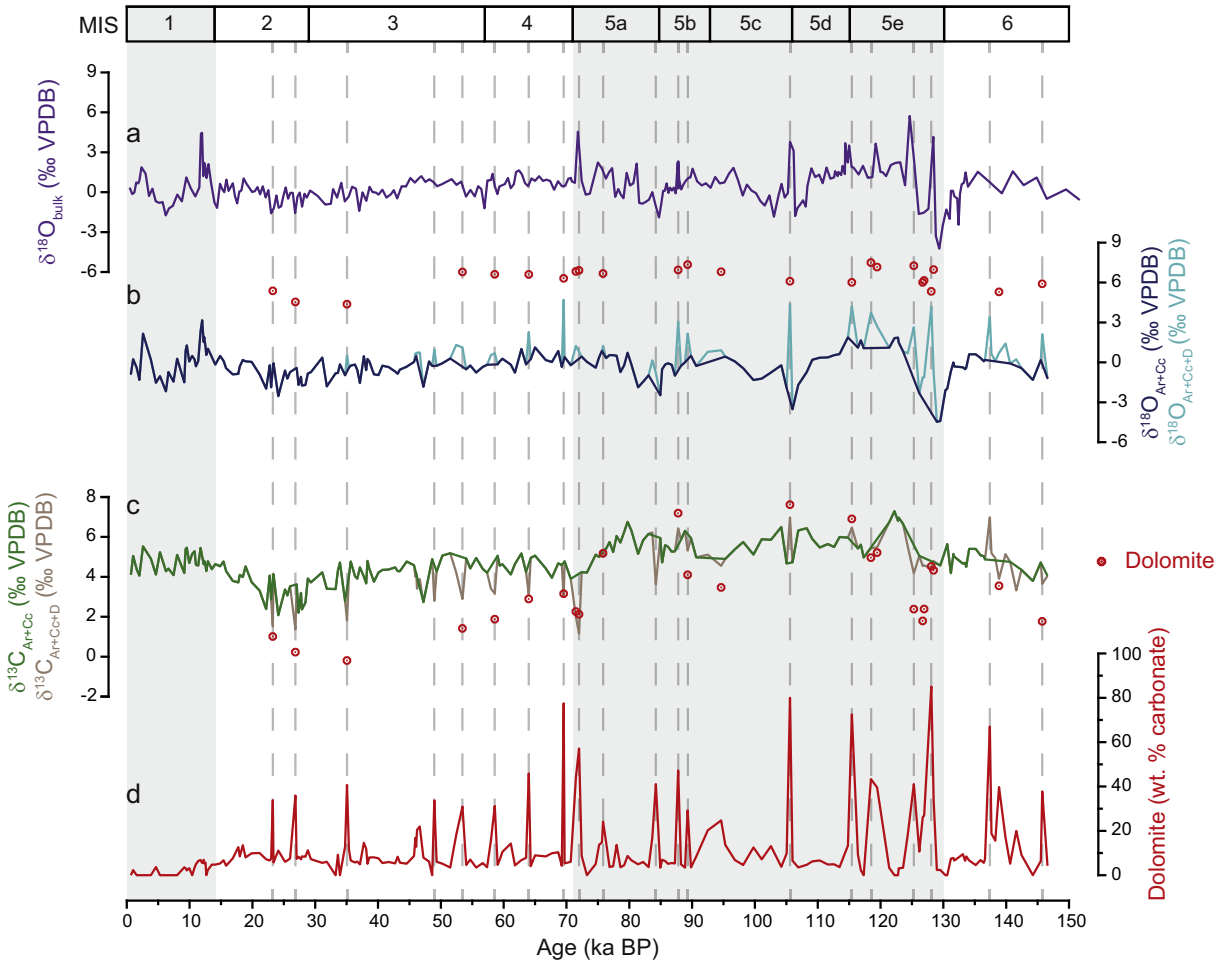

Fig. 5. Influence of dolomite on the bulk and fine fraction isotopic composition (Ar + Cc + D). a) Bulk oxygen isotope composition from Kwiecien et al. (2014). b) $\delta^{18}O$ record of fine fraction material (< 63 µm) after sieving ($\delta^{18}O_{Ar+Cc+D}$), dolomite-poor samples (< 15% dolomite; $\delta^{18}O_{Ar+Cc}$), and $\delta^{18}O$ values of isolated dolomite from McCormack et al. (2018). c) $\delta^{13}C$ record of fine fraction material ($\delta^{13}C_{Ar+Cc+D}$), $\delta^{13}C$ record of dolomite poor samples (< 15% dolomite; $\delta^{13}C_{Ar+Cc}$), and $\delta^{13}C$ values of isolated dolomite from McCormack et al. (2018). d) Concentration of calcian dolomite relative to aragonite and calcite (McCormack et al., 2018). Grey shaded areas represent Marine Isotope Stages (MIS) 1 and 5. The influence of dolomite on the isotopic signals of $\delta^{18}O_{bulk}$, $\delta^{18}O_{Ar+Cc+D}$, $\delta^{13}C_{Ar+Cc+D}$ is clearly visible for dolomite-rich samples.

from the climatically highly distinct periods 15.4–70.7 ka BP (Last Glacial) and 0–11.4 ka BP (Holocene) have very similar mean $\delta^{18}O_{Ar+Cc}$ values of −0.5 and –0.3‰ respectively. The $\delta^{13}C_{Ar+Cc}$ data show a higher variability between mean Last Glacial (3.9‰) and Holocene (4.7‰) values (Fig. 5c). In addition, the $\delta^{13}C_{Ar+Cc}$ record closely resembles the (Ar/(Ar + Cc) ratio, with higher (Ar / (Ar + Cc) ratios typically correlating to higher $\delta^{13}C_{Ar+Cc}$ (Figs. 6e, d, 7a).

6. Discussion

6.1. Mineralogy

6.1.1. Origin of carbonate minerals

Calcian dolomite in Lake Van sediments occurs episodically in significant concentrations, primarily within lake-level highstand deposits. Specifically, authigenic calcian dolomites are precipitated diagenetically within the pore space near the sediment-water interface (McCormack et al., 2018). The consistently low abundance of a possibly stoichiometric dolomite (ordering reflections could not be confirmed due to low XRD intensity) and the rare presence of coccoliths point to an insignificant contribution of detrital material. The crystal morphology of the euhedral $CaCO_3$ minerals including equant and prismatic calcite crystals (Fig. 4c, d) suggests that aragonite and the vast majority of calcite crystals most likely precipitated in the surface water. Similarly, the uniform small size of calcite crystals suggests precipitation within the water column (Murphy et al., 2014) rather than the sediment. In the further discussion we work under the assumption that calcite and aragonite precipitate within the surface water (epilimnion) and, at least for most of the record, settle to the lake bottom mostly unaltered.

6.1.2. Mechanism of aragonite and calcite precipitation

The seasonal character of varved Holocene sediments and the observed seasonality of whitings in modern Lake Van, combined with electron microprobe and CRM results allowed us to revise the different models proposed for carbonate precipitation (Table 1). Electron microprobe analyses of varved sediments highlight couplets of Ca-rich light and Si-Mg-rich dark laminae (laminae colouring is reversed under transmitted light) (Fig. 2a,b). CRM analyses document that calcite is the main carbonate constituent within the Si-Mg-rich laminae, while aragonite dominates the Ca-rich laminae (Fig. 2g). Strontium is more easily incorporated into the aragonite than calcite crystal structure (Lorens, 1981), therefore Sr distribution maps can also be tentatively used to visualise aragonite dominance within the Ca-rich layers (Fig. 2e). These observations suggest a stepwise precipitation of the respective polymorphs in the surface water, in agreement with the seasonally separated (spring and late summer) phases of whitings observed in Lake Van (Landmann and Kempe, 2002; Kempe and Kazmierczak, 2003;

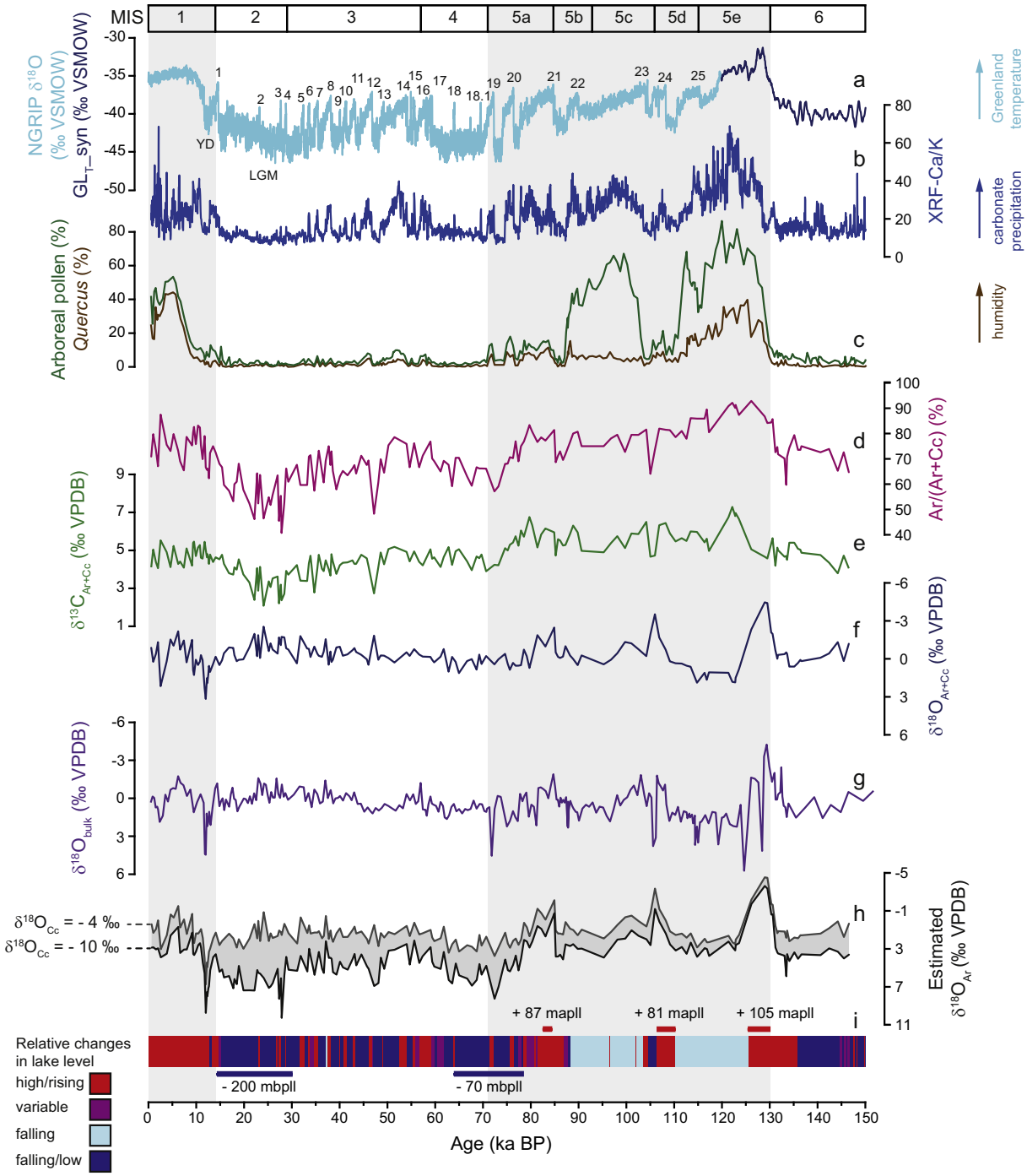

Fig. 6. Variations in the aragonite content and isotopic composition of aragonite-calcite mixed samples. a) Isotopic composition of the NGRIP ice core (NGRIP members et al., 2004; Steffensen et al., 2008; Svensson et al., 2008; Wolff et al., 2010) and a synthetic Greenland record (GLT_syn) (Barker et al., 2011). Sedimentary proxies from Lake Van include (b) XRF-Ca/K ratio (Kwiecien et al., 2014) and (c) arboreal pollen and *Quercus* pollen percentage (Litt et al., 2014; Pickarski et al., 2015a, 2015b; Pickarski and Litt, 2017). d) Relative aragonite content of dolomite poor samples (< 15% dolomite) expressed by an aragonite/non-dolomite ratio Ar / (Ar + Cc) in weight %. e, f) isotopic composition of dolomite poor samples ($\delta^{13}C_{Ar+Cc}$ and $\delta^{18}O_{Ar+Cc}$). g) Bulk carbonate oxygen isotope composition from Kwiecien et al. (2014). h) Estimated $\delta^{18}O_{Ar}$ values for $\delta^{18}O_{Cc}$ values between −4 and –10‰. i) Lithology-based relative lake-level changes (simplified after Stockhecke et al., 2014a) and major lake-level variations (Stockhecke et al., 2014a; Tomonaga et al., 2017) in metre above/below present lake level (mapll/mbpll). A comparison of $\delta^{18}O_{bulk}$ (g) with the estimated $\delta^{18}O_{Ar}$ record (h) illustrates the impact of the individual isotopic composition of the different mineral phases on the bulk isotopy.

Stockhecke et al., 2012) and with a model for calcite precipitation in Lake Van proposed by Landmann et al. (1996) and Lemcke (1996) explaining its formation despite the lake's high Mg/Ca ratio. Accordingly, calcite may precipitate above a chemocline, near the river mouths, observable as whitings created by the inflow of freshwater (with a lower Mg/Ca ratio) into the saline lake water. Calcite precipitating under these close-to-freshwater conditions will settle together with the siliciclastic (Si-Mg-rich) material (Fig. 2d, g, i) supplied to the lake via the same freshwater inflow. This scenario describes spring and late autumn whitings concomitant with increased river runoff. We speculate that whitings in late summer and early autumn (Landmann and Kempe, 2002; Kempe and Kazmierczak, 2003;

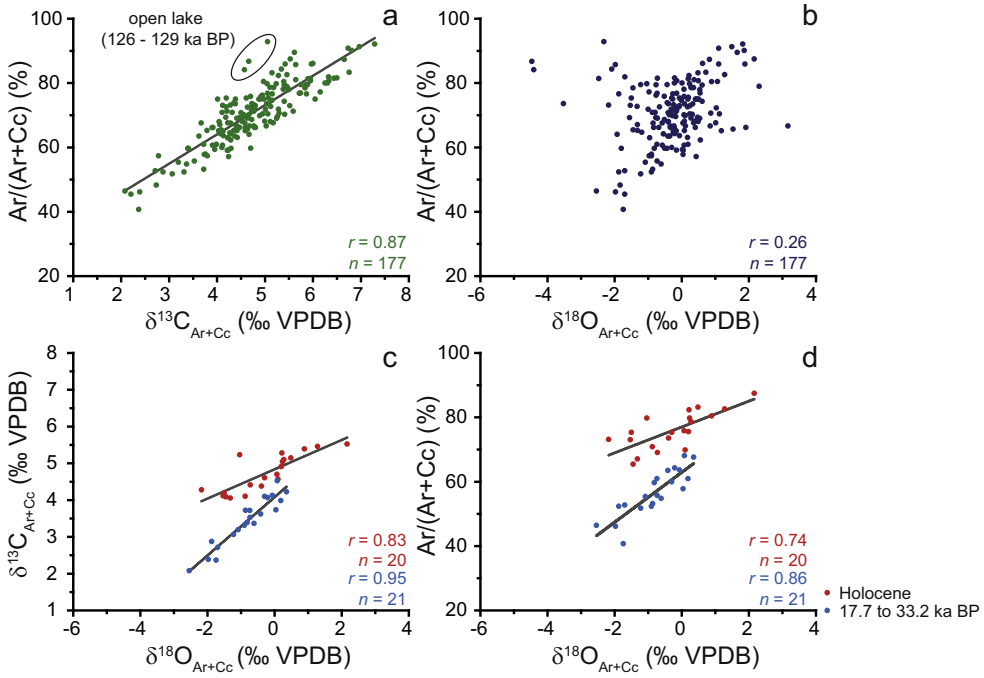

Fig. 7. a, b) Comparison between relative aragonite content of dolomite-poor samples and their isotopic composition. The three encircled samples are from the period (129–126 ka BP) in which Lake Van likely had an outflow. c) $\delta^{13}C_{Ar+Cc}$ vs. $\delta^{18}O_{Ar+Cc}$ and d) d) Ar / (Ar + Cc) vs. $\delta^{18}O_{Ar+Cc}$ for selected periods of low lithological variability. Holocene samples (0.6 to 11.4 ka BP, from finely laminated clayey silts) in red, and Last Glacial samples (15.5 to 33.2 ka BP) in blue. Intercalations of finely laminated layers were excluded here for Last Glacial samples. r is the correlation coefficient and n is the number of samples. (For interpretation of the references to colour in this figure legend, the reader is referred to the web version of this article.)

Stockhecke et al., 2012) are related to evapoconcentration and perhaps phytoplankton activity (Huguet et al., 2011; Stockhecke et al., 2012) and represent the precipitation of aragonite. With low detrital input (significantly reduced river runoff), late summer laminae consist mainly of aragonite (Fig. 2c, e, g, h). The presented model of spatial and temporal differences in calcite and aragonite precipitation stems from a critical review of the published concepts (Table 1), our new, detailed high-resolution observations (Fig. 2) and common-sense principles. Our predictions can be evaluated for their propriety in future research, optimally involving seasonally-resolved lake water chemistry coupled with sediment trap monitoring.

6.1.3. Aragonite and calcite precipitation on glacial/interglacial timescales

In the presence of high Mg/Ca ratios, magnesium ions inhibit calcite growth while aragonite growth is not affected (Mucci and Morse, 1983; Zhang and Dawe, 2000; Davis et al., 2000; De Choudens-Sánchez and González, 2009; Astilleros et al., 2010). An increase in aragonite precipitation relative to calcite in lacustrine environments is therefore commonly interpreted as an increase in the Mg/Ca ratio of the lake water, and consequently related to increased salinity associated with enhanced evaporation and a lower lake level (e.g. Spencer et al., 1984; Digerfeldt et al., 2000; Ülgen et al., 2012; Murphy et al., 2014). In Lake Van, periods of higher salinity and lower lake level (Stockhecke et al., 2014a; Tomonaga et al., 2017) result from decreased moisture availability during the Last Glacial period (Litt et al., 2014; Pickarski et al., 2015a, 2015b) and are characterised by commonly lower Ar / (Ar + Cc) values (Fig. 6d). In turn, rising/high lake levels (Landmann et al., 1996; Lemcke and Sturm, 1997; Wick et al., 2003; Kwiecien et al., 2014; Stockhecke et al., 2014a; Cukur et al., 2014; Çağatay et al., 2014) coincide with increasing aragonite concentration during the last 150 kyr (Fig. 6d, i). High aragonite concentrations also mark a possible open lake period at the beginning of MIS 5e (Stockhecke et al., 2014a; Tomonaga et al., 2017; North et al., 2017). Apparently, mechanisms other than lake water Mg/Ca ratio alone control changes in $CaCO_3$ polymorph precipitation in Lake Van.

Roeser et al. (2016) discussed selective dissolution of aragonite driven by aerobic metabolisation of organic matter within the sediment under prolonged exposure to oxygen to explain aragonite/calcite ratios in Lake Iznik. For Lake Van, however, aragonite concentrations are as high within sediments deposited during periods of a falling lake level with apparent oxygenated bottom waters (e.g. portions of MIS 5) as they are during suboxic/anoxic bottom water conditions (e.g. MIS 1) (Fig. 6d, i). In line with the model for seasonally/temporally separate aragonite and calcite precipitation in Lake Van, we favour the idea of climatic controlled variations in aragonite and calcite precipitation as the main control on Ar / (Ar + Cc) rather than selective dissolution of aragonite.

Accordingly, higher Ar / (Ar + Cc) content may be a result of enhanced seasonality and warmer summer temperatures (Fig. 6a, d). During interglacial periods, warmer conditions in the Eastern Mediterranean led to increased meteoric precipitation but also higher evaporation rates in summer (Jones and Roberts, 2008; Pickarski et al., 2015a). Analogous to modern conditions (Kaden et al., 2010; Huguet et al., 2011; Stockhecke et al., 2012) warmer summer temperatures would result in the formation of a seasonally stratified upper water column. Enhanced evaporation rates and possibly high productivity within the stratified surface water eventually leads to carbonate supersaturation and due to the lake waters high Mg/Ca ratio, aragonite precipitation. In contrast, aragonite precipitation might have been reduced during glacials/stadials. If generally colder glacial/stadial temperatures translate to longer/cooler winters and shorter/cooler summers, then the peak runoff (due to meltwater) would occur later in the year, summer surface water stratification would be decreased or shorter, and productivity likely lower. An increase in glacial/stadial spring/summer precipitation relative to winter (Orland et al., 2012; Rowe et al., 2012) would have the same effect, leading to calcite precipitation later in the year and lowering evaporative aragonite precipitation. Within these scenarios less carbonate would generally precipitate in the surface water and lower Ar / (Ar + Cc) content would be recorded for glacial and stadial conditions.

6.2. Carbon and oxygen isotope geochemistry

6.2.1. Influence of dolomite isotope signatures on the bulk sediment geochemistry

The similarity between both $\delta^{18}O_{bulk}$ and $\delta^{18}O_{Ar+Cc+D}$ argues that the different preparation methods used did not significantly influence either record. Although biogenic carbonates (ostracod valves) were not

removed from the bulk record, they do not noticeably influence the $\delta^{18}O_{bulk}$ record, as apparent from the similarity between the bulk and $\delta^{18}O_{Ar+Cc+D}$ record (from which ostracod valves were removed by wet sieving). Minor variations between the records result from resampling off-section and composite material at varying sampling depths and resolution (Fig. 5a, b).

A systematic approach testing the influence of secondary (dolomite, siderite) or detrital carbonates on bulk isotopy is rare in lacustrine research (e.g. Leng et al., 2010; Mangili et al., 2010; Lacey et al., 2015; McCormack et al., 2018). In Lake Van, dolomite is present more frequently and in larger abundances than previous mineralogical studies suggested (Landmann et al., 1996; Çağatay et al., 2014). Early diagenetic calcian dolomite precipitating within the pore space in the upper sediment column differs significantly from the primary surface water carbonates in terms of its isotopic signal (Fig. 5). Dolomite has consistently high $\delta^{18}O$ values (+4.4 to +7.5‰) resulting from its precipitation in cold, deep water and highly variable $\delta^{13}C$ values (−0.2 to +7.6‰) likely related to the involvement, at least to some degree, of microbial metabolism (McCormack et al., 2018). Distinct positive excursions in the $\delta^{18}O_{bulk}$ ($\delta^{18}O_{Ar+Cc+D}$) and variable excursions in the $\delta^{13}C_{Ar+Cc+D}$ coinciding with high dolomite concentrations (e.g. during MIS5e) are in good agreement with dolomite-related isotope geochemistry affecting these isotope records (Fig. 5).

6.2.2. Isotopic composition of sedimentary coeval aragonite and calcite

Due to the effects of evaporation in closed lakes, both the $\delta^{18}O_{lake}$ and the $\delta^{13}C_{DIC}$ are often enriched by > 10 to 15‰ relative to inflowing river water (Horton et al., 2016). Consequently, the revised calcite and aragonite precipitation model for Lake Van, under close-to-freshwater conditions and within evapoconcentrated lake water respectively, predicts strong variations between the individual isotopic compositions of each polymorph.

The aragonite content of the inorganically precipitated calcium carbonate polymorphs (Ar / (Ar + Cc)) strongly correlates with their carbon isotope composition ($\delta^{13}C_{Ar+Cc}$) (Fig. 7a). The aragonite and calcite oxygen isotope composition ($\delta^{18}O_{Ar+Cc}$) appears to show no such correlation (Fig. 7b). The $\delta^{13}C_{Ar+Cc}$ of the primary carbonates reflects the $\delta^{13}C_{DIC}$ within the lake's epilimnion at the time of crystallisation (Leng and Marshall, 2004). Lacustrine $\delta^{13}C_{DIC}$ is controlled mainly by three processes: atmosphere-water CO_2 exchange, the $\delta^{13}C_{DIC}$ of inflowing water and biological activity in the lake, i.e. photosynthesis and recycling of organic matter (Kelts and Talbot, 1990; Leng and Marshall, 2004). The enrichment of ^{13}C in aragonite in comparison to calcite ($\delta^{13}C_{Ar+Cc}$ spread between 2‰ for aragonite-poor and > 7‰ for aragonite-rich samples, Fig. 7a) cannot solely be explained by carbon isotope fractionation between aragonite and calcite, with aragonite being approximately 1.6 to 1.8‰ more positive than calcite when utilising the same DIC pool (Rubinson and Clayton, 1969; Turner, 1982; Romanek et al., 1992). Further, aragonite- and calcite-DIC $\delta^{13}C$ fractionation at temperatures between 10 and 40 °C is temperature independent (Romanek et al., 1992). While varying precipitation rates for both phases may alter the ^{13}C enrichment in aragonite with respect to calcite (Turner, 1982; Frisia et al., 2002; i.e. fractionation effects are more pronounced under slow precipitation rates) they cannot explain the large difference of approximately 11‰ between extrapolated aragonite (approximately 8‰) and calcite (approximately −3‰) endmembers (Fig. 7a). These observations are supported by the higher concentration of aragonite in the carbonate laminae within varved sediments (Fig. 2 g) and imply that aragonite and calcite in Lake Van did not utilise the same DIC pool during precipitation. Changes in $\delta^{13}C_{Ar+Cc}$ are therefore inherently related to changing Ar / (Ar + Cc) content (Figs. 6d, e, 7a).

Changing P/E ratios may have only minor effects on Lake Van's $\delta^{13}C_{DIC}$ signature because of the insensitivity of $\delta^{13}C_{DIC}$ values from large DIC pools to lake volume changes (Li and Ku, 1997). In contrast to $\delta^{13}C_{DIC}$, $\delta^{18}O$ values of the lake and runoff waters and of precipitating carbonates are expected to vary markedly with changes in the P/E ratio, variations in $\delta^{18}O$ values of the meteoric precipitation ($\delta^{18}O_P$) and temperature. As a consequence, on the whole, carbonate $\delta^{18}O_{Ar+Cc}$ shows no covariance with the Ar / (Ar + Cc) content (Fig. 7b) and $\delta^{13}C_{Ar+Cc}$ values (not shown) although the lake was closed for most of the time interval dealt with in this paper. On much shorter timescales, however, during periods with less pronounced temperature and lake level fluctuations, characterised by periods of low lithological variability, $\delta^{18}O_{Ar+Cc}$ does covary with $\delta^{13}C_{Ar+Cc}$ (Fig. 7c) and the Ar / (Ar + Cc) content (Fig. 7d). The surface water carbonates deposited mainly within banded clayey silts in the period of 17.7 to 33.2 ka BP (including the Last Glacial Maximum (LGM)) show a very strong covariance between $\delta^{18}O_{Ar+Cc}$ and $\delta^{13}C_{Ar+Cc}$ (Fig. 7c) and a strong covariance between $\delta^{18}O_{Ar+Cc}$ and Ar / (Ar + Cc) content (Fig. 7d). Accordingly, $\delta^{18}O_{Ar+Cc}$ values here are also influenced by the respective sample's aragonite and calcite content. Similar to carbon isotope fractionation between both polymorphs and DIC, the differences in oxygen isotope aragonite-water and calcite-water fractionation factors (approximately 0.6‰, Tarutani et al., 1969) alone are insufficient to explain the observed changes in amplitude (> 4‰, Fig. 7d). In conclusion, $\delta^{13}C$ and $\delta^{18}O$ values of aragonite are significantly higher than those of penecontemporary calcite.

6.2.3. Controls on aragonite and calcite $\delta^{13}C$ and $\delta^{18}O$ values

According to the revised model, calcite precipitates under freshwater influence, preserving a less evolved (closer to inflowing water) isotopic signal compared to aragonite, with $\delta^{18}O$ and $\delta^{13}C$ closer to those of freshwater runoff values. The $\delta^{18}O$ signature of calcite ($\delta^{18}O_{Cc}$) is influenced by the ^{18}O depleted $\delta^{18}O$ signature of meteoric precipitation ($\delta^{18}O_P$) and snowmelt controlling the $\delta^{18}O$ value of river water entering Lake Van (−11.5 and –10.1‰ VSMOW, Faber, 1978). In contrast, aragonite precipitating in late summer and early autumn from an evapoconcentrated stratified surface layer has an ^{18}O enriched oxygen isotope composition ($\delta^{18}O_{Ar}$) (Fig. 7d) mainly controlled by the isotopic composition of the lake water ($\delta^{18}O_{lake}$). Similarly, Dean et al. (2013) interpreted large differences between Lake Nar water $\delta^{18}O$ values estimated from sedimentary coeval diatoms and from carbonates as a result of the former precipitating within a surface freshwater layer and the latter in more evolved lake water.

Runoff $\delta^{13}C_{DIC}$ values are mainly controlled by isotopically light soil water carbon (Leng and Marshall, 2004) and dissolution of hinterland limestones in the catchment area. For carbonates precipitating near Ahlat Ridge, the dissolution of the Miocene Adilcevaz limestone ($\delta^{13}C$ of approximately 1‰, Çağatay et al., 2014) to the northwest of Lake Van may be of particular importance. Following the linear correlation between Ar / (Ar + Cc) content and $\delta^{13}C_{Ar+Cc}$ values (Fig. 7a), the Lake Van calcite endmember ($\delta^{13}C_{Cc}$) shows the expected low $\delta^{13}C$ values (approximately −3‰). In comparison, the estimated $\delta^{13}C$ value of aragonite ($\delta^{13}C_{Ar}$) is in the range of approximately 8‰ (Fig. 7a). Considering an aragonite-bicarbonate fractionation factor of about 2.7‰, as proposed by Romanek et al. (1992), aragonite precipitates from a DIC pool with a $\delta^{13}C_{DIC}$ signature of around 5‰. The $\delta^{13}C_{DIC}$ values for Lake Van are reported to be 3.4 to 5.5‰ in the surface water and 5.2 to 5.9‰ in the hypolimnion (Kempe et al., 1990). Lower surface water values (2.7‰) were reported by Lemcke (1996). The higher values reported by Kempe et al. (1990) are in the range of values expected for a simple inorganic aragonite precipitation within the lake water. Seasonally $^{13}C_{DIC}$-enriched values in the surface water mass may occur due to mixing with deeper water following destabilisation of the close-to-freshwater layer or photosynthetic activity within a summer stratified surface layer as observed in several lakes including Lake Greifen (Hollander and McKenzie, 1991), Lake Lugano (Lehmann et al., 2004), Lake Mendota (Hollander and Smith, 2001) and Lake Ontario (Hodell and Schelske, 1998). Similarly, Lake Van surface water $\delta^{13}C_{DIC}$ may increase to a level comparable to those reported for the hypolimnion or even higher in late summer and early autumn when basin

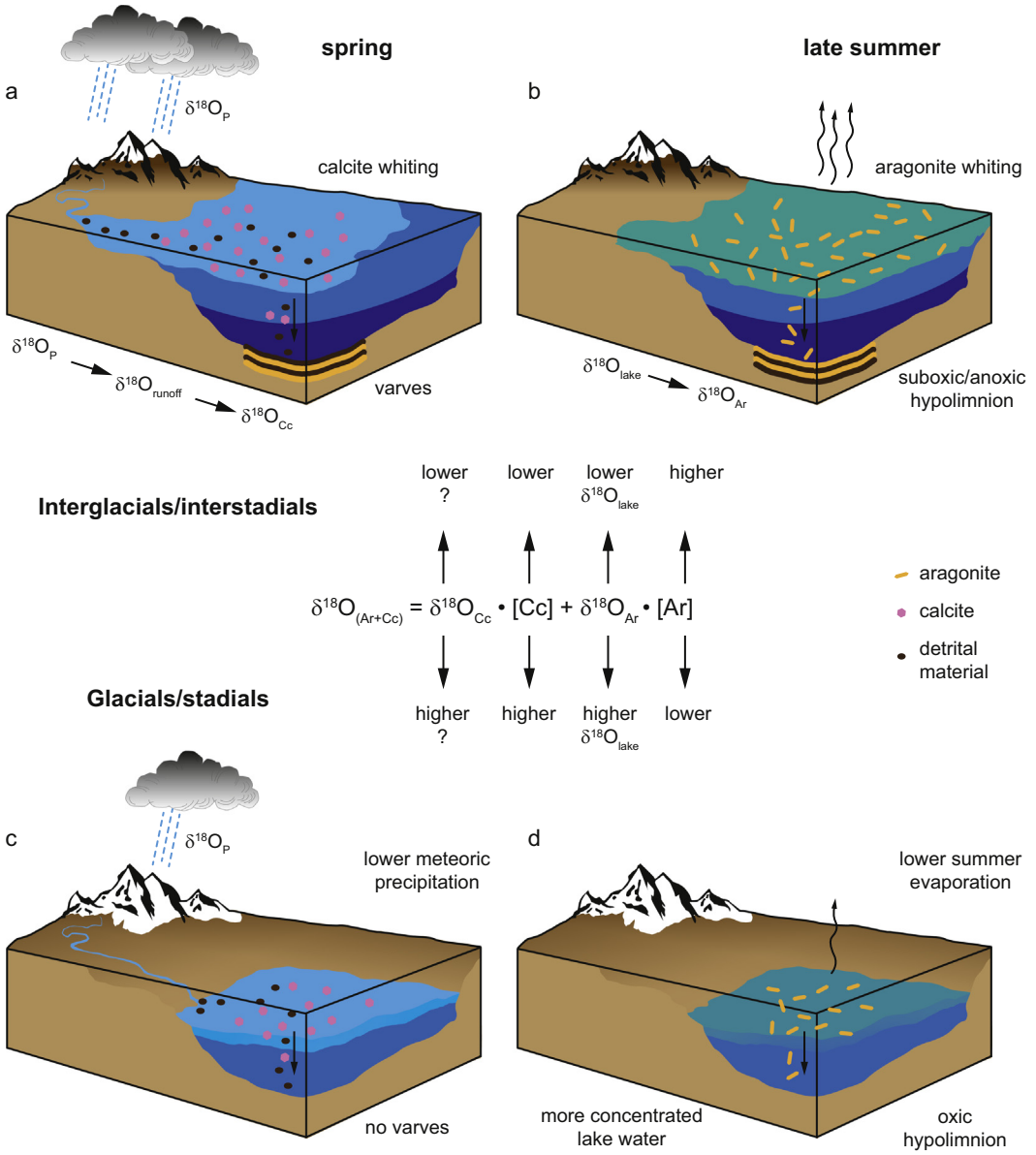

Fig. 8. Model of calcite and aragonite precipitation in Lake Van at annual resolution and on Interglacial/Glacial timescales. a) Calcite precipitates (river plume whitings) as freshwater enters the lake predominantly in spring (during high lake level interglacials/interstadials). Calcite and detrital material will settle together to form dark laminae. $\delta^{18}O$ values of calcite ($\delta^{18}O_{Cc}$) are strongly runoff ($\delta^{18}O_{runoff}$) and thereby meteoric precipitation ($\delta^{18}O_P$) influenced. b) Aragonite precipitates in late summer due to evapoconcentration and perhaps productivity (during high lake level interglacials/interstadials). Aragonite settles forming carbonate (aragonite) rich light laminae. $\delta^{18}O$ values of aragonite ($\delta^{18}O_{Ar}$) are strongly lake water ($\delta^{18}O_{lake}$) and perhaps surface water evaporation influenced. Varves are preserved when the lake level is high or rising, due to suboxic/anoxic bottom water conditions. c) Reduced runoff leads to a lower lake level, lower carbonate content, but a higher relative calcite content. d) Lower summer evaporation and productivity lead to lower aragonite content. A lower lake level implies higher $\delta^{18}O_{lake}$ and consequently higher $\delta^{18}O_{Ar}$ values. No varves are preserved during a low/falling lake level. $\delta^{18}O_{Ar+Cc}$ is expressed as $\delta^{18}O_{Ar} * [Ar] + \delta^{18}O_{Cc} * [Cc]$, whereas [Ar] and [Cc] are the relative concentrations of aragonite and calcite.

wide whitings (Landmann et al., 1996; Kempe and Kazmierczak, 2003; Reimer et al., 2009; Stockhecke et al., 2012) evidence carbonate precipitation (precipitating as aragonite).

6.2.4. Aragonite and calcite $\delta^{13}C$ and $\delta^{18}O$ values on glacial/interglacial timescales

The bulk isotopic composition varies with changing Ar / (Ar + Cc) content, but also with changes in the respective isotopic composition of the water masses from which aragonite and calcite precipitate (Fig. 8). On glacial/interglacial (stadial/interstadial) timescales, $\delta^{13}C_{Ar+Cc}$ appears to be mainly reflecting changing Ar / (Ar + Cc) content (Fig. 6d, e, 7 a) implying low isotopic variability in the DIC of the lake water ($\delta^{13}C_{Ar}$) and runoff ($\delta^{13}C_{Cc}$). Still, lower vegetation density during colder/drier periods (Kwiecien et al., 2014; Pickarski et al., 2015a, 2015b), may have resulted in higher runoff $\delta^{13}C_{DIC}$ leading to higher $\delta^{13}C_{Cc}$ values, while atmosphere-water CO_2 exchange and phototrophic activity are potentially important for $\delta^{13}C_{Ar}$ values. Nevertheless, the influence of these environmental factors will likely be less pronounced due to the high DIC content in both the tributaries and the lake (Reimer et al., 2009).

In contrast to $\delta^{13}C_{Ar+Cc}$, controls on $\delta^{18}O_{Ar+Cc}$ appear more complex (Figs. 6f, 7b). Mean Holocene $\delta^{18}O_{Ar+Cc}$ values (−0.27‰, ± 1.1‰) are similar to mean Last Glacial values (−0.45‰, ± 0.7‰), while Ar / (Ar + Cc) content differs markedly (Fig. 6d, f). The $\delta^{18}O$ values of both polymorphs may vary over glacial/interglacial timescales due to carbonate-water temperature-dependent

fractionation (Craig, 1965). Pending that the above considerations are correct, precipitation of calcite in the close-to-freshwater layer would take place at temperatures likely not varying significantly over the millennia. Changes in $\delta^{18}O$ values of the respective parent waters are therefore a significantly more important factor for the oxygen isotope composition of calcite and aragonite (Fig. 8).

The $\delta^{18}O$ values of calcite precipitating under close-to-freshwater conditions will largely reflect variations in $\delta^{18}O_{runoff}$ values and consequently the oxygen isotope composition of meteoric precipitation and snowmelt. On glacial/interglacial and stadial/interstadial timescales, $\delta^{18}O_P$ values depend on temperature (Dansgaard relationship), the source area, the amount effect and the seasonality of meteoric precipitation. Mean annual $\delta^{18}O_P$ is positively correlated with temperature (Dansgaard, 1964). In the Mediterranean region, however, this correlation is less pronounced (+0.2‰ °C^{-1}, Bard et al., 2002) compared to mid-high latitudes (+0.6‰ °C^{-1}, Rozanski et al., 1992). In contrast, many continental Mediterranean carbonate records tend to have higher glacial than interglacial $\delta^{18}O$ values partly explained by the source area effect (Frumkin et al., 1999; Kolodny et al., 2005; Roberts et al., 2008). In short, the higher LGM global oceanic $\delta^{18}O$ signature (Schrag et al., 2002) is paralleled and amplified in the Eastern Mediterranean Sea (Vergnaud Grazzini et al., 1986; Bigg, 1995; Frumkin et al., 1999; Emeis et al., 2000) leading to higher LGM $\delta^{18}O_P$ values (Kolodny et al., 2005; Roberts et al., 2008). Changes in rainfall amount may also on glacial/interglacial timescales, influence $\delta^{18}O_P$ with lower values during periods of enhanced rainfall (interglacials) (e.g. Bar-Matthews et al., 2003). An increase in spring/summer (higher $\delta^{18}O_P$) relative to winter (lower $\delta^{18}O_P$) meteoric precipitation may also lead to higher $\delta^{18}O$ values in glacial continental carbonate records (Orland et al., 2012; Rowe et al., 2012). The net effect of these partially interdependent controls on $\delta^{18}O_P$ may imply generally higher $\delta^{18}O_P$ values during glacials relative to interglacials (e.g. Frumkin et al., 1999; Bar-Matthews et al., 2003; Roberts et al., 2008; Orland et al., 2012; Rowe et al., 2012).

The isotopic composition of aragonite has generally a larger influence on $\delta^{18}O_{Ar+Cc}$ in Lake Van compared to that of calcite, as aragonite is typically the dominant polymorph (Fig. 6d). The $\delta^{18}O_{Ar}$ value will primarily reflect $\delta^{18}O_{lake}$, which is typically enriched relative to the $\delta^{18}O_{runoff}$ it originates from (Horton et al., 2016). For hydrologically closed lakes changes in the P/E ratio are the most important influence on the $\delta^{18}O_{lake}$ signature (Leng and Marshall, 2004). However, increased evaporation rates volumetrically limited to the relatively thin epilimnion could also cause an enrichment in ^{18}O limited to the stratified surface layer (i.e., higher than average $\delta^{18}O_{lake}$). The sensitivity of $\delta^{18}O_{Ar}$ values towards the P/E ratio is highlighted for the onset of MIS 5e (130.6–126.2 ka BP), a period in which Lake Van may have been an open lake (Stockhecke et al., 2014a; Tomonaga et al., 2017; North et al., 2017). Despite high aragonite content (84–93%), $\delta^{18}O_{Ar+Cc}$ and $\delta^{13}C_{Ar+Cc}$ display relative low values of −2 to −4.5‰ and 4.6 to 5.6‰ respectively (Figs. 6, 7a). With an increase in freshwater inflow and the establishment of an outflow, the residence time of water within a lake is significantly reduced. This leads to a stronger influence of freshwater $\delta^{18}O_{runoff}$ (ultimately reflecting $\delta^{18}O_P$ values) on the oxygen isotope composition of carbonates precipitating in the lake (Talbot, 1990; Leng and Marshall, 2004). The $\delta^{18}O_{Ar}$ value is much more depleted (i.e. less evolved) during hydrologically open periods of Lake Van, as opposed to periods of hydrological closure.

Similarly, the establishment of an outflow, explaining the preservation of otherwise absent diatoms within MIS 5e sediments (North et al., 2017), would have resulted in a reduction of the lakes total DIC content and less alkaline conditions. Due to the lower DIC content of the open lake, lake water $\delta^{13}C_{DIC}$ values might have been more influenced by lower runoff $\delta^{13}C_{DIC}$, leading to lower $\delta^{13}C$ values of aragonite (Fig. 7a, 'open lake' samples). Moreover, atmospheric CO_2 exchange with the lake water may be severely reduced following a rapid increase in lake volume, which could also lead to lower $\delta^{13}C_{DIC}$ values (Li and Ku, 1997). Interestingly, despite the open lake (freshwater or close-to-freshwater) conditions, aragonite is the main precipitate during this period. Typically, calcite is the most common $CaCO_3$ polymorph in freshwater environments. Yet, depending on the lake's chemistry (specifically the Mg/Ca ratio), aragonite can not only precipitate (e.g. Lake Balaton, Müller, 1971) but also dominate surface water precipitation (Lake Kivu, Votava et al., 2017) in freshwater lakes. The Mg/Ca ratio in the open Lake Van water masses was apparently still high enough for aragonite precipitation, likely due to the effective removal of Ca^{2+} and the longer residence time of Mg^{2+} (Reimer et al., 2009). Between 126 and 123 ka BP $\delta^{18}O_{Ar+Cc}$ and $\delta^{13}C_{Ar+Cc}$ isotope values become significantly higher while aragonite content remains high, likely indicating falling lake levels and re-establishment of a hydrological closed system.

In summary, $\delta^{18}O_{Ar+Cc}$ values can be expressed as $\delta^{18}O_{Ar+Cc} = \delta^{18}O_{Ar} * [Ar] + \delta^{18}O_{Cc} * [Cc]$ (Fig. 8). Where [Ar] and [Cc] are the relative frequencies of aragonite and calcite (for [Ar] + [Cc] = 1). To visualise the possible range in changes in $\delta^{18}O_{Ar}$ ($\delta^{18}O_{lake}$) we tentatively estimated changes in $\delta^{18}O_{Ar}$ following this equation by assuming a likely range of values for $\delta^{18}O_{Cc}$. Modern $\delta^{18}O$ values of river water entering Lake Van are between −11.5 and –10.1‰ VSMOW (Faber, 1978), while early summer lake surface water $\delta^{18}O$ is between −0.4 and 1‰ VSMOW (Kempe et al., 1990; Jasechko et al., 2013). Assuming a surface water temperature of approximately 10 °C in spring (Kaden et al., 2010; Stockhecke et al., 2012) and applying the fractionation factor from Kim and O'Neil (1997), calcite precipitating solely out of the runoff would have a $\delta^{18}O$ value of approximately −10‰, whereas a calcite precipitating from a 50% mixture of lake and runoff water $\delta^{18}O$ should yield a value of approximately −4‰. Applying these boundary conditions for $\delta^{18}O_{Cc}$ (−4 to −10‰) yielded a possible range of $\delta^{18}O_{Ar}$ (Fig. 6h). The estimated $\delta^{18}O_{Ar}$ values are results of several assumptions and may be compromised as a result of the absence modern seasonally resolved water chemistry data and due to $\delta^{18}O_{Cc}$ values beyond the assumed range, the uncertainty in relative carbonate concentration based on the RIR method, larger variations in temperature at the time of calcite precipitation or minor contributions of detrital and/or diagenetic carbonates to the $\delta^{18}O_{Ar+Cc}$ values. Still, the estimated $\delta^{18}O_{Ar}$ signature clearly shows significantly lower values during periods of a high lake level, especially during MIS 5 (Fig. 6h) and higher values during periods of a low lake level, such as the particularly dry YD (Stockhecke et al., 2014a). If interpreted in the traditional way (e.g. Leng and Marshall, 2004), the higher $\delta^{18}O_{bulk}$ and $\delta^{18}O_{Ar+Cc}$ values within MIS 5 (Fig. 6f, g) point to generally drier conditions (i.e. lower P/E ratios) during MIS 5 in comparison to the Last Glacial period. Such interpretation contrasts a large array of Lake Van proxy records (Kwiecien et al., 2014; Litt et al., 2014; Stockhecke et al., 2014a; Pickarski et al., 2015a, 2015b; Pickarski and Litt, 2017; Randlett et al., 2017; Tomonaga et al., 2017). Following the assumed boundary conditions, the estimated $\delta^{18}O_{Ar}$ values, point to generally wetter climate (lower values) during MIS 5 concurring with the arboreal pollen record (Fig. 6c, Litt et al., 2014; Pickarski et al., 2015a, 2015b; Pickarski and Litt, 2017), the XRF-Ca/K ratio (Fig. 6b, Kwiecien et al., 2014) and the lithology (Fig. 6i, Stockhecke et al., 2014a). Similar to our estimated $\delta^{18}O_{Ar}$ record for interglacials (MIS 1 and 5), the generally higher glacial values (particularly for calcite precipitation under low mixture with lake water) are also in line with a glacial aridity increase as indicated by non-carbonate based proxy records (Fig. 6).

The $\delta^{18}O_{Ar+Cc}$ record in Lake Van is ultimately controlled by the complex interaction between the relative concentration of each polymorph and centennial to millennial scale variations in the isotopic composition of aragonite and calcite source waters (Fig. 8).

6.2.5. Broader implications for lakes where calcite and/or aragonite are precipitating in the surface water

The Lake Van data document the possibility of

penecontemporaneous nucleation and growth of calcite and aragonite from the epilimnion under different geochemical conditions. These polymorphs, with distinct geochemical signatures, may subsequently be deposited coeval or close to coeval in a sedimentary record.

While the presence of both polymorphs is not uncommon in lacustrine sediments, to our knowledge no study dealing with lake archives has considered mineralogy-dependent isotopic variability other than the respectively different isotopic fractionation factors. The mineralogy of carbonates is an inherent function of the environmentally-controlled water chemistry. Processes changing the water chemistry in favour of a specific carbonate mineral, will also influence its isotopic composition. Our example testifies that, if singled out, the isotopic composition of different penecontemporaneous polymorphs can record spatially and temporally different processes. In the particular case of Lake Van, the isotopic composition of calcite is indicative of changes in the isotopic composition of meteoric precipitation and freshwater-lake water mixing processes. In contrast, the isotopic signature of aragonite reflects changing evaporation/precipitation ratios and likely lake water CO_2 exchange and productivity.

7. Conclusions

In contrast to a wide array of independent proxy records previously recovered from the 2010 ICDP PALEOVAN project, bulk carbonate $\delta^{18}O$ was an equivocal recorder of environmental changes. Here we analysed material covering the last 150 kyr and performed a comprehensive mineralogy-specific oxygen and carbon isotope study. Mineralogically, Lake Van's inorganic carbonate inventory consists of (i) variable amounts of surface water precipitates (aragonite and low-magnesium calcite) and (ii) calcian dolomite forming in the pore space close to the sediment-water interface.

The application of confocal Raman microscopy and electron microprobe analyses, allowed us to revise a seasonally and spatially separated model for carbonate formation in Lake Van. Further, the aid of high-resolution XRD data and isotope analyses, enabled the expansion of the revised model to glacial/interglacial and stadial/interstadial time scales:

(1) The high-resolution investigation of annually laminated sediments suggests that nucleation and precipitation of both, aragonite and low-magnesium calcite respectively, takes place in the surface water but seems to be temporally and spatially separated.
(2) Calcite precipitates under close-to-freshwater conditions (river plume whitings mainly in spring) while aragonite precipitates in late summer. Accordingly, the isotope signatures of calcite are strongly freshwater influenced (^{18}O and ^{13}C depleted) compared to the evapoconcentrated lake water isotopy (^{18}O and ^{13}C enriched) recorded in aragonite.
(3) The $\delta^{18}O$ and $\delta^{13}C$ values from mixed aragonite and calcite-bearing samples ($\delta^{18}O_{Ar+Cc}$, $\delta^{13}C_{Ar+Cc}$) record an isotopically mixed signal shifted towards the dominant polymorph. Ignoring the mixed nature of carbonates in lacustrine sediments and/or ignoring the isotopic differences of both polymorphs can severally compromise palaeoclimate interpretations.
(4) Early diagenetic (authigenic) dolomite is characterised by high $\delta^{18}O$ and non-systematically variable $\delta^{13}C$ values and occurs episodically and volumetrically significant in Lake Van sediments and where this is the case, induces a bias in the bulk isotope record.
(5) Bulk sediment $\delta^{18}O$ and $\delta^{13}C$ values in Lake Van are therefore controlled by the relative concentration of the carbonate mineral phases (aragonite, calcite, dolomite) and their respective isotopic signals. The isotopic composition of surface water carbonates is affected by the hydrological conditions of its precipitation environment. Both the relative concentration of aragonite and calcite as well as the isotopic composition of their respective source waters change independently from each other on glacial/interglacial and stadial/interstadial timescales.
(6) The isotope composition of samples containing unspecified amounts of aragonite and calcite is commonly corrected, if at all, only for the different fractionation factors. We postulate that a generalised assumption of sedimentary coeval calcite and aragonite precipitating from water with the same isotopic composition is flawed. The application of the revised hydrologically-separated calcite/aragonite precipitation model introduced here will refine environmental reconstructions and help avoiding equivocal interpretations based on bulk carbonate archives.

Acknowledgements

We acknowledge funding from the Deutsche Forschungsgemeinschaft (DFG) grant KW90/2-1. We are grateful to Sebastian Breitenbach, Thomas Reinecke, and Rolf Neuser for instrumental assistance, and appreciate the assistence of Julian Stromann and Annabel Wolf with the sample preparation. The manuscript benefited from the thorough and constructive feedback of the editor Michael Böttcher and two anonymous reviewers.

References

Astilleros, J.M., Fernández-Díaz, L., Putnis, A., 2010. The role of magnesium in the growth of calcite: an AFM study. Chem. Geol. 271 (1), 52–58. https://doi.org/10.1016/j.chemgeo.2009.12.011.

Bard, E., Delaygue, G., Rostek, F., Antonioli, F., Silenzi, S., Schrag, D.P., 2002. Hydrological conditions over the western Mediterranean basin during the deposition of the cold Sapropel 6 (ca. 175 kyr BP). Earth Planet. Sci. Lett. 202 (2), 481–494. https://doi.org/10.1016/S0012-821X(02)00788-4.

Barker, S., Knorr, G., Edwards, R.L., Parrenin, F., Putnam, A.E., Skinner, L.C., Wolff, E., Ziegler, M., 2011. 800,000 years of abrupt climate variability. Science 334 (6054), 347–351. https://doi.org/10.1126/science.1203580.

Bar-Matthews, M., Ayalon, A., Gilmour, M., Matthews, A., Hawkesworth, C.J., 2003. Sea–land oxygen isotopic relationships from planktonic foraminifera and speleothems in the Eastern Mediterranean region and their implication for paleorainfall during interglacial intervals. Geochim. Cosmochim. Acta 67 (17), 3181–3199. https://doi.org/10.1016/S0016-7037(02)01031-1.

Bernasconi, S.M., McKenzie, J.A., 2013. Lake sediments. In: Elias, S.A. (Ed.), Encyclopedia of Quaternary Science, 2. Elsevier, Amsterdam, pp. 333–340.

Bigg, G.R., 1995. Aridity of the Mediterranean Sea at the last glacial maximum: a reinterpretation of the $\delta^{18}O$ record. Paleoceanography 10 (2), 283–290. https://doi.org/10.1029/94PA03165.

Breitenbach, S.F., Bernasconi, S.M., 2011. Carbon and oxygen isotope analysis of small carbonate samples (20 to 100 μg) with a GasBench II preparation device. Rapid Commun. Mass Spectrom. 25 (13), 1910–1914. https://doi.org/10.1002/rcm.5052.

Burton, E.A., Walter, L.M., 1987. Relative precipitation rates of aragonite and Mg calcite from seawater: Temperature or carbonate ion control? Geology 15 (2), 111–114. https://doi.org/10.1130/0091-7613(1987)15<111:RPROAA>2.0.CO;2.

Çağatay, M.N., Öğretmen, N., Damcı, E., Stockhecke, M., Sancar, Ü., Eriş, K.K., Özeren, S., 2014. Lake level and climate records of the last 90 ka from the Northern Basin of Lake Van, eastern Turkey. Quat. Sci. Rev. 104, 97–116. https://doi.org/10.1016/j.quascirev.2014.09.027.

Craig, H., 1965. The measurement of oxygen isotope palaeotemperatures. In: Tongiorgi, E. (Ed.), Stable Isotopes in Oceanographic Studies and Palaeotemperatures. Pisa, Consiglio Nazionale delle Ricerche Laboratorio di Geologia Nucleare, pp. 161–182.

Cukur, D., Krastel, S., Schmincke, H.U., Sumita, M., Tomonaga, Y., Çağatay, M.N., 2014. Water level changes in Lake Van, Turkey, during the past ca. 600 ka: climatic, volcanic and tectonic controls. J. Paleolimnol. 52 (3), 201–214. https://doi.org/10.1007/s10933-014-9788-0.

Dansgaard, W., 1964. Stable isotopes in precipitation. Tellus 16 (4), 436–468. https://doi.org/10.3402/tellusa.v16i4.8993.

Davis, K.J., Dove, P.M., De Yoreo, J.J., 2000. The role of Mg^{2+} as an impurity in calcite growth. Science 290 (5494), 1134–1137. https://doi.org/10.1126/science.290.5494.1134.

De Choudens-Sánchez, V., González, L.A., 2009. Calcite and aragonite precipitation under controlled instantaneous supersaturation: elucidating the role of $CaCO_3$ saturation state and Mg/Ca ratio on calcium carbonate polymorphism. J. Sediment. Res. 79 (6), 363–376. https://doi.org/10.2110/jsr.2009.043.

Dean, J.R., Jones, M.D., Leng, M.J., Sloane, H.J., Roberts, C.N., Woodbridge, J., Swann, G.E.A., Metcalfe, S.E., Eastwood, W.J., Yiğitbaşıoğlu, H., 2013. Palaeo-seasonality of the last two millennia reconstructed from the oxygen isotope composition of carbonates and diatom silica from Nar Gölü, central Turkey. Quat. Sci. Rev. 66, 35–44. https://doi.org/10.1016/j.quascirev.2012.07.014.

Dean, J.R., Jones, M.D., Leng, M.J., Noble, S.R., Metcalfe, S.E., Sloane, H.J., Sahy, D., Eastwood, W.J., Roberts, C.N., 2015. Eastern Mediterranean hydroclimate over the late glacial and Holocene, reconstructed from the sediments of Nar lake, central Turkey, using stable isotopes and carbonate mineralogy. Quat. Sci. Rev. 124, 162–174. https://doi.org/10.1016/j.quascirev.2015.07.023.

Degens, E.T., Wong, H.K., Kempe, S., Kurtman, F., 1984. A geological study of Lake Van, eastern Turkey. Geol. Rundsch. 73 (2), 701–734. https://doi.org/10.1007/BF01824978.
Deocampo, D.M., 2010. The geochemistry of continental carbonates. Dev. Sedimentol. 62, 1–59. https://doi.org/10.1016/S0070-4571(09)06201-3.
Digerfeldt, G., Olsson, S., Sandgren, P., 2000. Reconstruction of lake-level changes in lake Xinias, central Greece, during the last 40,000 years. Palaeogeogr. Palaeoclimatol. Palaeoecol. 158 (1), 65–82. https://doi.org/10.1016/S0031-0182(00)00029-8.
Emeis, K.C., Struck, U., Schulz, H.M., Rosenberg, R., Bernasconi, S., Erlenkeuser, H., Sakamoto, T., Martinez-Ruiz, F., 2000. Temperature and salinity variations of Mediterranean Sea surface waters over the last 16,000 years from records of planktonic stable oxygen isotopes and alkenone unsaturation ratios. Palaeogeogr. Palaeoclimatol. Palaeoecol. 158 (3), 259–280. https://doi.org/10.1016/S0031-0182(00)00053-5.
Faber, E., 1978. $^{18}O/^{16}O$ and D/H analyses on waters from Lake Van area. In Geology of Lake Van. ed. Degens E.T. & Kurtmann F. Miner Res Explor Inst Turkey 169, 45–49.
Fernández-Diaz, L., Putnis, A., Prieto, M., Putnis, C.V., 1996. The role of magnesium in the crystallization of calcite and aragonite in a porous medium. J. Sediment. Res. 66 (3).
Frisia, S., Borsato, A., Fairchild, I.J., McDermott, F., Selmo, E.M., 2002. Aragonite-calcite relationships in speleothems (Grotte de Clamouse, France): environment, fabrics, and carbonate geochemistry. J. Sediment. Res. 72 (5), 687–699. https://doi.org/10.1306/020702720687.
Frumkin, A., Ford, D.C., Schwarcz, H.P., 1999. Continental oxygen isotopic record of the last 170,000 years in Jerusalem. Quat. Res. 51 (3), 317–327. https://doi.org/10.1006/qres.1998.2031.
Goldsmith, J.R., Graf, D.L., Heard, H.C., 1961. Lattice constants of the calcium-magnesium carbonates. Am. Mineral. 46 (3–4), 453–457.
González, L. A., & Lohmann, K. C. (1988). Controls on mineralogy and composition of spelean carbonates: Carlsbad Caverns, New Mexico. In Paleokarst (pp. 81-101). Springer New York. doi:https://doi.org/10.1007/978-1-4612-3748-8_4.
Hodell, D.A., Schelske, C.L., 1998. Production, sedimentation, and isotopic composition of organic matter in Lake Ontario. Limnol. Oceanogr. 43 (2), 200–214. https://doi.org/10.4319/lo.1998.43.2.0200.
Hollander, D.J., McKenzie, J.A., 1991. CO_2 control on carbon-isotope fractionation during aqueous photosynthesis: a paleo-pCO_2 barometer. Geology 19 (9), 929–932. https://doi.org/10.1130/0091-7613(1991)019<0929:CCOCIF>2.3.CO;2.
Hollander, D.J., Smith, M.A., 2001. Microbially mediated carbon cycling as a control on the $\delta^{13}C$ of sedimentary carbon in eutrophic Lake Mendota (USA): new models for interpreting isotopic excursions in the sedimentary record. Geochim. Cosmochim. Acta 65 (23), 4321–4337. https://doi.org/10.1016/S0016-7037(00)00506-8.
Horton, T.W., Defliese, W.F., Tripati, A.K., Oze, C., 2016. Evaporation induced ^{18}O and ^{13}C enrichment in lake systems: a global perspective on hydrologic balance effects. Quat. Sci. Rev. 131, 365–379. https://doi.org/10.1016/j.quascirev.2015.06.030.
Huguet, C., Fietz, S., Stockhecke, M., Sturm, M., Anselmetti, F.S., Rosell-Mele, A., 2011. Biomarker seasonality study in Lake Van, Turkey. Org. Geochem. 42 (11), 1289–1298. https://doi.org/10.1016/j.orggeochem.2011.09.007.
Irion, G., 1973. Die anatolischen Salzseen, ihr Chemismus und die Entstehung ihrer chemischen Sedimente. Arch. Hydrobiol. 71 (4), 517–557.
Jasechko, S., Sharp, Z.D., Gibson, J.J., Birks, S.J., Yi, Y., Fawcett, P.J., 2013. Terrestrial water fluxes dominated by transpiration. Nature 496 (7445), 347. https://doi.org/10.1038/nature11983.
Jones, M.D., Roberts, C.N., 2008. Interpreting lake isotope records of Holocene environmental change in the Eastern Mediterranean. Quat. Int. 181 (1), 32–38. https://doi.org/10.1016/j.quaint.2007.01.012.
Kaden, H., Peeters, F., Lorke, A., Kipfer, R., Tomonaga, Y., Karabiyikoglu, M., 2010. Impact of lake level change on deep-water renewal and oxic conditions in deep saline Lake Van, Turkey. Water Resour. Res. 46 (11). https://doi.org/10.1029/2009WR008555.
Kelts, K., Talbot, M., 1990. Lacustrine carbonates as geochemical archives of environmental change and biotic/abiotic interactions. In: Tilzer, M.M., Serruya, C. (Eds.), Large Lakes: Ecological Structure and Function. Science Technical Publications, Madison, pp. 290–317. https://doi.org/10.1007/978-3-642-84077-7_15.
Kempe, S., & Kazmierczak, J. (2003). Modern soda lakes: model environments for an early alkaline ocean. Modelling in natural sciences; design, validation and case studies. Springer, Berlin, 309-322.
Kempe, S., Landmann, G., Konuk, T., & Düzbastilar, M. (1990). Berichte zur 3. Internationalen Van See Expedition 7. Juni bis 6. Juli 1990. 10.13140/RG.2.2.12966.93767.
Kempe, S., Kazmierczak, J., Landmann, G., Konuk, T., Reimer, A., Lipp, A., 1991. Largest known microbialites discovered in Lake Van, Turkey. Nature 349 (6310), 605–608. https://doi.org/10.1038/349605a0.
Khoo, F., Degens, E.T., Lambert, A., 1978. Geochemistry of Lake Van sediments. In Geology of Lake Van. ed. Degens E.T. & Kurtmann F. Miner Res Explor Inst Turkey 169, 81–91.
Kim, S.T., O'Neil, J.R., 1997. Equilibrium and nonequilibrium oxygen isotope effects in synthetic carbonates. Geochim. Cosmochim. Acta 61 (16), 3461–3475.
Kolodny, Y., Stein, M., Machlus, M., 2005. Sea-rain-lake relation in the Last Glacial East Mediterranean revealed by $\delta^{18}O$-$\delta^{13}C$ in Lake Lisan aragonites. Geochim. Cosmochim. Acta 69 (16), 4045–4060. https://doi.org/10.1016/j.gca.2004.11.022.
Kwiecien, O., Stockhecke, M., Pickarski, N., Heumann, G., Litt, T., Sturm, M., Anselmetti, F., Kipfer, R., Haug, G.H., 2014. Dynamics of the last four glacial terminations recorded in Lake Van, Turkey. Quat. Sci. Rev. 104, 42–52. https://doi.org/10.1016/j.quascirev.2014.07.001.
Lacey, J.H., Leng, M.J., Francke, A., Sloane, H.J., Milodowski, A., Vogel, H., Baumgarten, H., Wagner, B., 2015. Mediterranean climate since the Middle Pleistocene: a 640 ka stable isotope record from Lake Ohrid (Albania/Macedonia). Biogeosci. Discuss. 12 (16), 13427–13481. https://doi.org/10.5194/bgd-12-13427-2015.
Landmann, G., Kempe, S., 2002. Seesedimente als Klimaarchiv—Fallbeispiele: Van See und Totes Meer. Angewandte Geowissenschaften in Darmstadt. Schriftenr Dt Geol Ges 15, 129–143.
Landmann, G., Reimer, A., Kempe, S., 1996. Climatically induced lake level changes at Lake Van, Turkey, during the Pleistocene/Holocene transition. Glob. Biogeochem. Cycles 10 (4), 797–808. https://doi.org/10.1029/96GB02347.
Lehmann, M.F., Bernasconi, S.M., McKenzie, J.A., Barbieri, A., Simona, M., Veronesi, M., 2004. Seasonal variation of the $\delta^{13}C$ and $\delta^{15}N$ of particulate and dissolved carbon and nitrogen in Lake Lugano: Constraints on biogeochemical cycling in a eutrophic lake. Limnol. Oceanogr. 49 (2), 415–429. https://doi.org/10.4319/lo.2004.49.2.0415.
Lemcke, G., 1996. Paläoklimarekonstruktion am Van See (Ostanatolien, Türkei). Doctoral dissertation, ETH Zürich, 182 pp., unpublished.
Lemcke, G., Sturm, M., 1997. $\delta^{18}O$ and Trace Element Measurements as Proxy for the Reconstruction of Climate Changes at Lake Van (Turkey): Preliminary Results. In Third Millennium BC Climate Change and Old World Collapse (Pp. 653–678) Springer, Berlin Heidelberg. https://doi.org/10.1007/978-3-642-60616-8_29.
Leng, M.J., Marshall, J.D., 2004. Palaeoclimate interpretation of stable isotope data from lake sediment archives. Quat. Sci. Rev. 23 (7), 811–831. https://doi.org/10.1016/j.quascirev.2003.06.012.
Leng, M.J., Jones, M.D., Frogley, M.R., Eastwood, W.J., Kendrick, C.P., Roberts, C.N., 2010. Detrital carbonate influences on bulk oxygen and carbon isotope composition of lacustrine sediments from the Mediterranean. Glob. Planet. Chang. 71 (3–4), 175–182. https://doi.org/10.1016/j.gloplacha.2009.05.005.
Li, H.C., Ku, T.L., 1997. $\delta^{13}C$–$\delta^{18}C$ covariance as a paleohydrological indicator for closed-basin lakes. Palaeogeogr. Palaeoclimatol. Palaeoecol. 133 (1), 69–80. https://doi.org/10.1016/S0031-0182(96)00153-8.
Litt, T., Anselmetti, F.S., 2014. Lake Van deep drilling project PALEOVAN. Quat. Sci. Rev. 104, 1–7. https://doi.org/10.1016/j.quascirev.2014.09.026.
Litt, T., Anselmetti, F.S., Baumgarten, H., Beer, J., Cagatay, N., Cukur, D., Damci, E., Glombitza, C., Haug, G., Heumann, G., Kallmeyer, J., Kipfer, R., Krastel, S., Kwiecien, O., Meydan, A.F., Orcen, S., Pickarski, N., Randlett, M.-E., Schmincke, H.-U., Schubert, C.J., Sturm, M., Sumita, M., Stockhecke, M., Tomonaga, Y., Vigliotti, L., Wonik, T., the PALEOVAN Scientific Team, 2012. 500,000 Years of environmental history in eastern Anatolia: the PALEOVAN drilling project. Sci. Drill. 14, 18–29. https://doi.org/10.5194/sd-14-18-2012.
Litt, T., Pickarski, N., Heumann, G., Stockhecke, M., Tzedakis, P.C., 2014. A 600,000 year long continental pollen record from Lake Van, eastern Anatolia (Turkey). Quat. Sci. Rev. 104, 30–41. https://doi.org/10.1016/j.quascirev.2014.03.017.
Lorens, R.B., 1981. Sr, Cd, Mn and Co distribution coefficients in calcite as a function of calcite precipitation rate. Geochim. Cosmochim. Acta 45 (4), 553–561. https://doi.org/10.1016/0016-7037(81)90188-5.
Lumsden, D.N., 1979. Discrepancy between thin-section and X-ray estimates of dolomite in limestone. J. Sediment. Res. 49 (2), 429–436.
Mangili, C., Brauer, A., Plessen, B., Dulski, P., Moscariello, A., Naumann, R., 2010. Effects of detrital carbonate on stable oxygen and carbon isotope data from varved sediments of the interglacial Pianico palaeolake (Southern Alps, Italy). J. Quat. Sci. 25 (2), 135–145. https://doi.org/10.1002/jqs.1282.
McCormack, J., Bontognali, T.R.R., Immenhauser, A., Kwiecien, O., 2018. Controls on cyclic formation of Quaternary early diagenetic dolomite. Geophys. Res. Lett. 45 (8), 3625–3634. https://doi.org/10.1002/2018GL077344.
Meckler, A.N., Ziegler, M., Millán, M.I., Breitenbach, S.F., Bernasconi, S.M., 2014. Long-term performance of the Kiel carbonate device with a new correction scheme for clumped isotope measurements. Rapid Commun. Mass Spectrom. 28 (15), 1705–1715. https://doi.org/10.1002/rcm.6949.
Morse, J.W., Wang, Q., Tsio, M.Y., 1997. Influences of temperature and Mg: Ca ratio on CaCO3 precipitates from seawater. Geology 25 (1), 85–87. https://doi.org/10.1130/0091-7613(1997)025<0085:IOTAMC>2.3.CO;2.
Mucci, A., Morse, J.W., 1983. The incorporation of Mg^{2+} and Sr^{2+} into calcite overgrowths: influences of growth rate and solution composition. Geochim. Cosmochim. Acta 47 (2), 217–233. https://doi.org/10.1016/0016-7037(83)90135-7.
Müller, G., 1971. Aragonite inorganic precipitation in a freshwater lake. Nat. Phys. Sci. 229 (1), 18. https://doi.org/10.1038/physci229018a0.
Müller, G., Irion, G., Förstner, U., 1972. Formation and diagenesis of inorganic Ca−Mg carbonates in the lacustrine environment. Naturwissenschaften 59 (4), 158–164.
Murphy, J.T., Lowenstein, T.K., Pietras, J.T., 2014. Preservation of primary lake signatures in alkaline earth carbonates of the Eocene Green River Wilkins Peak-Laney Member transition zone. Sediment. Geol. 314, 75–91. https://doi.org/10.1016/j.sedgeo.2014.09.005.
Mutlu, H., Güleç, N., Hilton, D.R., Aydın, H., Halldórsson, S.A., 2012. Spatial variations in gas and stable isotope compositions of thermal fluids around Lake Van: implications for crust–mantle dynamics in eastern Turkey. Chem. Geol. 300, 165–176. https://doi.org/10.1016/j.chemgeo.2012.01.026.
Nehrke, G., Nouet, J., 2011. Confocal Raman microscope mapping as a tool to describe different mineral and organic phases at high spatial resolution within marine biogenic carbonates: case study on Nerita undata (Gastropoda, Neritopsina). Biogeosciences 8 (12), 3761–3769. https://doi.org/10.5194/bg-8-3761-2011.
NGRIP members, Andersen, K.K., Azuma, N., Barnola, J.M., Bigler, M., Biscaye, P., Caillon, N., Chappellaz, J., Clausen, H.B., Dahl-Jensen, D., Fischer, H., Flückiger, J., Fritzsche, D., Fujii, Y., Goto-Azuma, K., Grønvold, K., Gundestrup, N.S., Hansson, M., Huber, C., Hvidberg, C.S., Johnsen, S.J., Jonsell, U., Jouzel, J., Kipfstuhl, S., Landais, A., Leuenberger, M., Lorrain, R., Masson-Delmotte, V., Miller, H., Motoyama, H., Narita, H., Popp, T., Rasmussen, S.O., Raynaud, D., Rothlisberger, R., Ruth, U., Samyn, D., Schwander, J., Shoji, H., Siggard-Andersen, M.-L., Steffensen, J.P., Stocker, T., Sveinbjörnsdóttir, A.E., Svensson, A., Takata, M., Tison, J.-L.,

Thorsteinsson, T., Watanabe, O., Wilhelms, F., White, J.W.C., 2004. High-resolution record of Northern Hemisphere climate extending into the last interglacial period. Nature 431 (7005), 147–151. https://doi.org/10.1038/nature02805.

North, S.M., Stockhecke, M., Tomonaga, Y., Mackay, A.W., 2017. Analysis of a fragmentary diatom record from Lake Van (Turkey) reveals substantial lake-level variability during previous interglacials MIS7 and MIS5e. J. Paleolimnol. 59 (1), 119–133. https://doi.org/10.1007/s10933-017-9973-z.

Orland, I.J., Bar-Matthews, M., Ayalon, A., Matthews, A., Kozdon, R., Ushikubo, T., Valley, J.W., 2012. Seasonal resolution of Eastern Mediterranean climate change since 34 ka from a Soreq Cave speleothem. Geochim. Cosmochim. Acta 89, 240–255. https://doi.org/10.1016/j.gca.2012.04.035.

Pickarski, N., Litt, T., 2017. A new high-resolution pollen sequence at Lake Van, Turkey: insights into penultimate interglacial–glacial climate change on vegetation history. Clim. Past 13 (6), 689. https://doi.org/10.5194/cp-13-689-2017.

Pickarski, N., Kwiecien, O., Djamali, M., Litt, T., 2015a. Vegetation and environmental changes during the last interglacial in eastern Anatolia (Turkey): a new high-resolution pollen record from Lake Van. Palaeogeogr. Palaeoclimatol. Palaeoecol. 435, 145–158. https://doi.org/10.1016/j.palaeo.2015.06.015.

Pickarski, N., Kwiecien, O., Langgut, D., Litt, T., 2015b. Abrupt climate and vegetation variability of eastern Anatolia during the last glacial. Clim. Past 11 (11), 1491–1505. https://doi.org/10.5194/cp-11-1491-2015.

Randlett, M.E., Bechtel, A., van der Meer, M.T., Peterse, F., Litt, T., Pickarski, N., Kwiecien, O., Stockhecke, M., Wehrli, B., Schubert, C.J., 2017. Biomarkers in Lake Van sediments reveal dry conditions in eastern Anatolia during 110.000–10.000 years BP. Geochem. Geophys. Geosyst. 18 (2), 571–583. https://doi.org/10.1002/2016GC006621.

Reimer, A., Landmann, G., Kempe, S., 2009. Lake Van, eastern Anatolia, hydrochemistry and history. Aquat. Geochem. 15 (1–2), 195–222. https://doi.org/10.1007/s10498-008-9049-9.

Roberts, N., Jones, M. D., Benkaddour, A., Eastwood, W. J., Filippi, M. L., Frogley, M. R., Lamb, H. F., Leng, M. J., Reed, J. M., Stein., M., Stevens, L., Valero-Garcés, B., & Zanchetta, G. (2008). Stable isotope records of Late Quaternary climate and hydrology from Mediterranean lakes: the ISOMED synthesis. Quat. Sci. Rev., 27(25), 2426–2441. doi:https://doi.org/10.1016/j.quascirev.2008.09.005.

Roeser, P., Franz, S.O., Litt, T., 2016. Aragonite and calcite preservation in sediments from Lake Iznik related to bottom lake oxygenation and water column depth. Sedimentology 63 (7), 2253–2277. https://doi.org/10.1111/sed.12306.

Romanek, C.S., Grossman, E.L., Morse, J.W., 1992. Carbon isotopic fractionation in synthetic aragonite and calcite: effects of temperature and precipitation rate. Geochim. Cosmochim. Acta 56 (1), 419–430. https://doi.org/10.1016/0016-7037(92)90142-6.

Rowe, P.J., Mason, J.E., Andrews, J.E., Marca, A.D., Thomas, L., Van Calsteren, P., Jex, C.N., Vonhof, H.B., Al-Omari, S., 2012. Speleothem isotopic evidence of winter rainfall variability in northeast Turkey between 77 and 6 ka. Quat. Sci. Rev. 45, 60–72. https://doi.org/10.1016/j.quascirev.2012.04.013.

Rozanski, K., Araguas-Araguas, L., Gonfiantini, R., 1992. Relation between long-term trends of oxygen-18 isotope composition of precipitation and climate. Science 258 (5084), 981–985. https://doi.org/10.1126/science.258.5084.981.

Rubinson, M., Clayton, R.N., 1969. Carbon-13 fractionation between aragonite and calcite. Geochim. Cosmochim. Acta 33 (8), 997–1002. https://doi.org/10.1016/0016-7037(69)90109-4.

Schrag, D.P., Adkins, J.F., McIntyre, K., Alexander, J.L., Hodell, D.A., Charles, C.D., McManus, J.F., 2002. The oxygen isotopic composition of seawater during the Last Glacial Maximum. Quat. Sci. Rev. 21 (1–3), 331–342. https://doi.org/10.1016/S0277-3791(01)00110-X.

Snyder, R.L., 1992. The use of reference intensity ratios in X-ray quantitative analysis. Powder Diffract. 7 (04), 186–193. https://doi.org/10.1017/S0885715600018686.

Spencer, R.J., Baedecker, M.J., Eugster, H.P., Forester, R.M., Goldhaber, M.B., Jones, B.F., Kelts, K., McKenzie, J., Madsen, D.B., Rettig, S.L., Rubin, M., Bowser, C.J., 1984. Great Salt Lake, and precursors, Utah: the last 30,000 years. Contrib. Mineral. Petrol. 86 (4), 321–334. https://doi.org/10.1007/BF01187137.

Steffensen, J.P., Andersen, K.K., Bigler, M., Clausen, H.B., Dahl-Jensen, D., Fischer, H., Goto-Azuma, K., Hansson, M., Johnson, S.J., Jouzel, J., Masson-Delmotte, V., Popp, T., Rasmussen, S.O., Röthlisberger, R., Ruth, U., Stauffer, B., Siggaard-Andersen, M.-L., Sveinbjörnsdóttir, A.E., Svensson, A., White, J.W.C., 2008. High-resolution Greenland ice core data show abrupt climate change happens in few years. Science 321 (5889), 680–684. https://doi.org/10.1126/science.1157707.

Stockhecke, M. (2008). The Annual Particle Cycle of Lake Van: Insights from Space, Sediments and the Water Column. M.S. Thesis. University of Zurich. 167 pp., unpublished.

Stockhecke, M., Anselmetti, F.S., Meydan, A.F., Odermatt, D., Sturm, M., 2012. The annual particle cycle in Lake Van (Turkey). Palaeogeogr. Palaeoclimatol. Palaeoecol. 333, 148–159. https://doi.org/10.1016/j.palaeo.2012.03.022.

Stockhecke, M., Sturm, M., Brunner, I., Schmincke, H.U., Sumita, M., Kipfer, R., Cukur, D., Kwiecien, O., Anselmetti, F.S., 2014a. Sedimentary evolution and environmental history of Lake Van (Turkey) over the past 600,000 years. Sedimentology 61 (6), 1830–1861. https://doi.org/10.1111/sed.12118.

Stockhecke, M., Kwiecien, O., Vigliotti, L., Anselmetti, F.S., Beer, J., Çağatay, M.N., Channell, J.E.T., Kipfer, R., Lachner, J., Litt, T., Pickarski, N., Sturm, M., 2014b. Chronostratigraphy of the 600,000 year old continental record of Lake Van (Turkey). Quat. Sci. Rev. 104, 8–17. https://doi.org/10.1016/j.quascirev.2014.04.008.

Svensson, A., Andersen, K.K., Bigler, M., Clausen, H.B., Dahl-Jensen, D., Davies, S.M., Johnsen, S.J., Muscheler, R., Parrenin, F., Rasmussen, S.O., Röthlisberger, R., Seierstad, I., Steffensen, J.P., Vinther, B.M., 2008. A 60,000 year Greenland stratigraphic ice core chronology. Clim. Past 4 (1), 47–57. https://doi.org/10.5194/cp-4-47-2008.

Talbot, M.R., 1990. A review of the palaeohydrological interpretation of carbon and oxygen isotopic ratios in primary lacustrine carbonates. Chemical Geology: Isotope Geoscience Section 80 (4), 261–279. https://doi.org/10.1016/0168-9622(90)90009-2.

Tarutani, T., Clayton, R.N., Mayeda, T.K., 1969. The effect of polymorphism and magnesium substitution on oxygen isotope fractionation between calcium carbonate and water. Geochim. Cosmochim. Acta 33 (8), 987–996. https://doi.org/10.1016/0016-7037(69)90108-2.

Tomonaga, Y., Brennwald, M.S., Livingstone, D.M., Kwiecien, O., Randlett, M.È., Stockhecke, M., Unwin, K., Anselmetti, F.S., Beer, J., Haug, G.H., Schubert, C.J., Sturm, M., Kipfer, R., 2017. Porewater salinity reveals past lake-level changes in Lake Van, the Earth's largest soda lake. Sci. Rep. 7, 1–10. https://doi.org/10.1038/s41598-017-00371-w.

Turner, J.V., 1982. Kinetic fractionation of carbon-13 during calcium carbonate precipitation. Geochim. Cosmochim. Acta 46 (7), 1183–1191. https://doi.org/10.1016/0016-7037(82)90004-7.

Ülgen, U.B., Franz, S.O., Biltekin, D., Çagatay, M.N., Roeser, P.A., Doner, L., Thein, J., 2012. Climatic and environmental evolution of Lake Iznik (NW Turkey) over the last ~4700 years. Quat. Int. 274, 88–101. https://doi.org/10.1016/j.quaint.2012.06.016.

Vergnaud Grazzini, C.V., Devaux, M., Znaidi, J., 1986. Stable isotope “anomalies” in Mediterranean Pleistocene records. Mar. Micropaleontol. 10 (1), 35–69. https://doi.org/10.1016/0377-8398(86)90024-1.

Votava, J.E., Johnson, T.C., Hecky, R.E., 2017. Holocene carbonate record of Lake Kivu reflects the history of hydrothermal activity. Proc. Natl. Acad. Sci. 114 (2), 251–256. https://doi.org/10.1073/pnas.1609112113.

Wick, L., Lemcke, G., Sturm, M., 2003. Evidence of Lateglacial and Holocene climatic change and human impact in eastern Anatolia: high-resolution pollen, charcoal, isotopic and geochemical records from the laminated sediments of Lake Van, Turkey. The Holocene 13 (5), 665–675. https://doi.org/10.1191/0959683603hl653rp.

Wolff, E.W., Chappellaz, J., Blunier, T., Rasmussen, S.O., Svensson, A., 2010. Millennial-scale variability during the last glacial: the ice core record. Quat. Sci. Rev. 29 (21), 2828–2838. https://doi.org/10.1016/j.quascirev.2009.10.013.

Yu J. Q., & Kelts, K.R. (2002). Abrupt changes in climatic conditions across the late-glacial/Holocene transition on the N. E. Tibet-Qinghai Plateau: evidence from Lake Qinghai, China. J. Paleolimnol., 28, 195–206, 2002. doi:https://doi.org/10.1023/A:1021635715857.

Zhang, Y., Dawe, R.A., 2000. Influence of Mg^{2+} on the kinetics of calcite precipitation and calcite crystal morphology. Chem. Geol. 163 (1), 129–138. https://doi.org/10.1016/S0009-2541(99)00097-2.